Counting photons, one-by-one…

a short walk in the world of photonics

Massimo Caccia
Uni. Insubria, Como, Italy
Massimo.Caccia@uninsubria.it

XXVII Giornate di Studio sui rivelatori – Cogne – February 15th, 2018

4 steps in the photonics world:

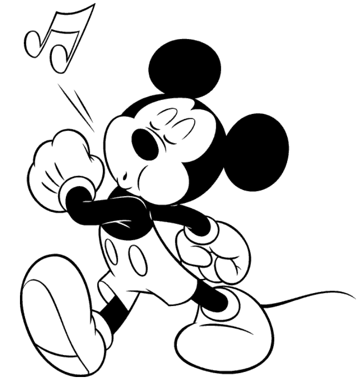

1. *Have you ever seen a photon? What can you do presuming to be able to see single photons?*

2. *Single Photon sensitive detectors for "daily" use:*
   - *yesterday [Photomultiplier tubes];*
   - ***today** [Single Photon Avalanche Photodiodes & Silicon Photomultipliers];*

3. *Silicon Photomultipliers: fundamentals, ☺ & ☹ , the way forward [integrated single photon sensitive microsystems]*

4. *Exemplary applications & demo*

Have you ever seen a Photon? [step 1]

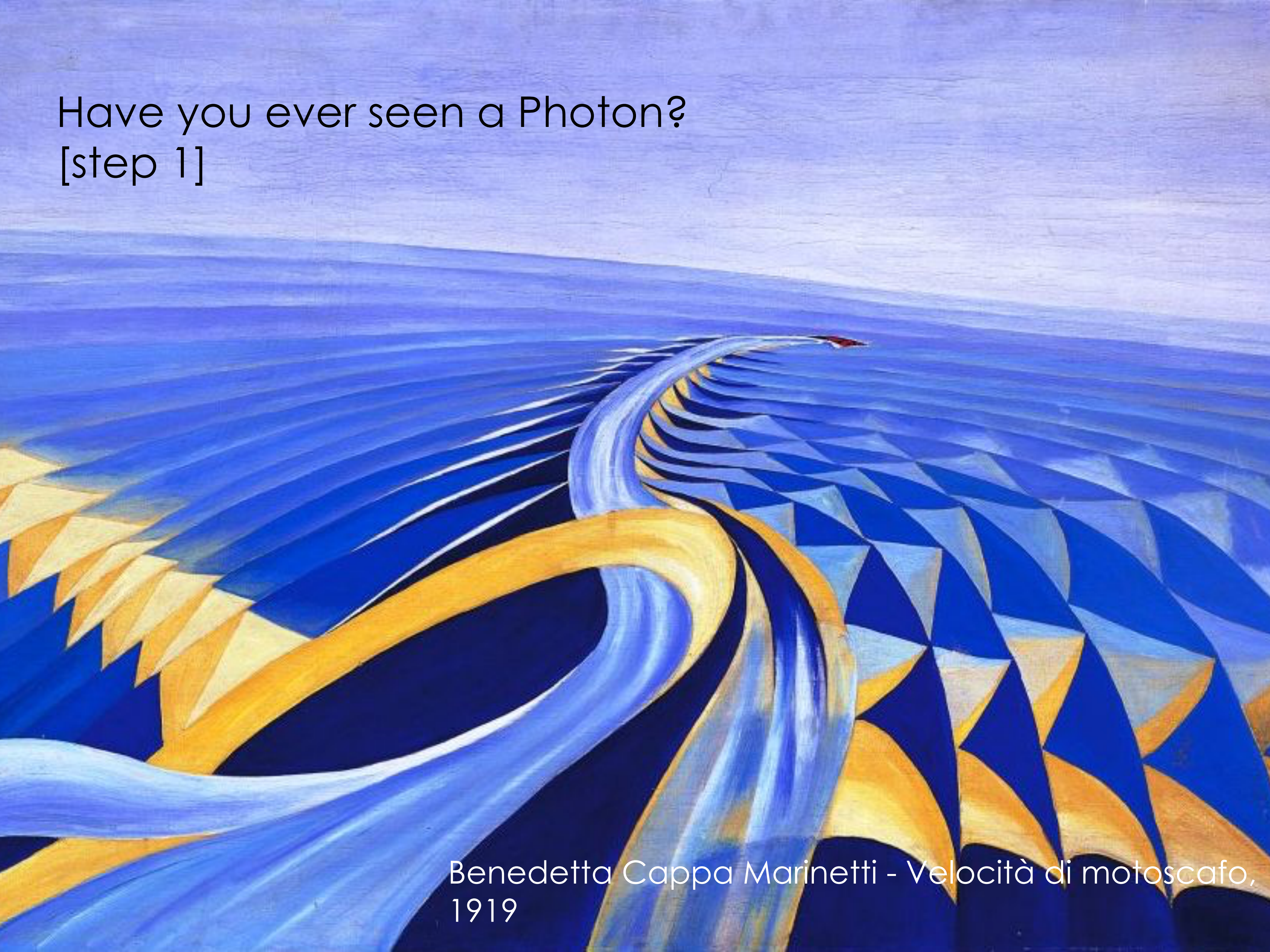

Benedetta Cappa Marinetti - Velocità di motoscafo, 1919

The Afghan Girl [Steve Mc Curry, 1984]

Eyes are possibly the best instruments ever created to see the light. Certainly, they represent the most beautiful way to see what we see…

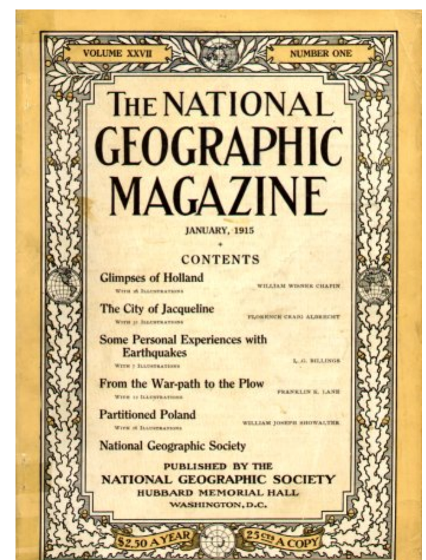

VOLUME XXVII NUMBER ONE

THE NATIONAL GEOGRAPHIC MAGAZINE

JANUARY, 1915

CONTENTS

Glimpses of Holland — WILLIAM WISNER CHAPIN

The City of Jacqueline — FLORENCE CRAIG ALBRECHT

Some Personal Experiences with Earthquakes — L. G. BILLINGS

From the War-path to the Plow — FRANKLIN K. LANE

Partitioned Poland — WILLIAM JOSEPH SHOWALTER

National Geographic Society

PUBLISHED BY THE NATIONAL GEOGRAPHIC SOCIETY
HUBBARD MEMORIAL HALL
WASHINGTON, D.C.

$2.50 A YEAR — 25 CTS A COPY

NGM cover, June 1985 & 2002

And not all of the eyes were made equal:

Of chickens & men:

- White curve: color sensitivity of the human eye
- Black curve: color sensitivity of a chicken eye

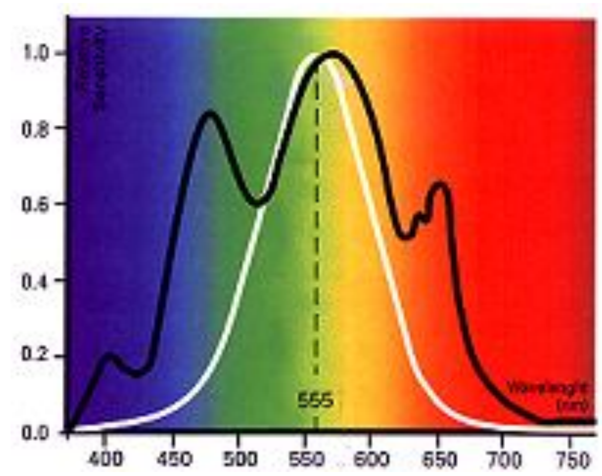

Vs.

Nature is offering us a beautiful variety of light sensitive devices:

Among them, I just want to pick up one example fitting our scope…

The owl eyes: a good example of natural instruments to gain an extended perception of reality

- 100 times more sensitive than a human eye
- If our night sky is full of 6000 stars, an owl can distinguish up to 1 000 000 stars

Can the owl see single photons?

But can a human being see a single photon?

ENERGY, QUANTA, AND VISION*

By SELIG HECHT, SIMON SHLAER, AND MAURICE HENRI PIRENNE‡
(From the Laboratory of Biophysics, Columbia University, New York)

(Received for publication, March 30, 1942)

TABLE II
Minimum Energy for Vision

Each datum is the result of many measurements during a single experimental period, and is the energy which can be seen with 60 per cent frequency. $\lambda = 510\ m\mu$; $h\nu = 3.84 \times 10^{-12}$ ergs.

Observer	Energy	No. of quanta	Observer	Energy	No. of quanta
	ergs $\times 10^{10}$			*ergs* $\times 10^{10}$	
S. H.	4.83	126	C. D. H.	2.50	65
	5.18	135		2.92	76
	4.11	107		2.23	58
	3.34	87		2.23	58
	3.03	79			
	4.72	123	M. S.	3.31	81
	5.68	148		4.30	112
S. S.	3.03	79	S. R. F.	4.61	120
	2.07	54			
	2.15	56	A. F. B.	3.19	83
	2.38	62			
	3.69	96	M. H. P.	3.03	79
	3.80	99		3.19	83
	3.99	104		5.30	138

It takes something between 54 and 138 photons to tell with 60% probability the flash was seen ⇒ dropping from 5-8 when the Poissonian property of the light source is accounted for

Whether humans can see single photons is an argument still being debated today:

nature COMMUNICATIONS

ARTICLE

Received 15 Jan 2016 | Accepted 7 Jun 2016 | Published 19 Jul 2016

DOI: 10.1038/ncomms12172

OPEN

Direct detection of a single photon by humans

Jonathan N. Tinsley[1,2,†,*], Maxim I. Molodtsov[1,2,3,*], Robert Prevedel[1,2,3], David Wartmann[1,†], Jofre Espigulé-Pons[2,4], Mattias Lauwers[1] & Alipasha Vaziri[1,2,3,5]

Despite investigations for over 70 years, the absolute limits of human vision have remained unclear. Rod cells respond to individual photons, yet whether a single-photon incident on the eye can be perceived by a human subject has remained a fundamental open question. Here we report that humans can detect a single-photon incident on the cornea with a probability significantly above chance. This was achieved by implementing a combination of a psychophysics procedure with a quantum light source that can generate single-photon states of light. We further discover that the probability of reporting a single photon is modulated by the presence of an earlier photon, suggesting a priming process that temporarily enhances the effective gain of the visual system on the timescale of seconds.

A quantum technology experimen!

So it is very likely an owl can see a photon; certainly, he can do a lot with its extended perception of reality…

What could we aim for, presuming to be able to see single photons?

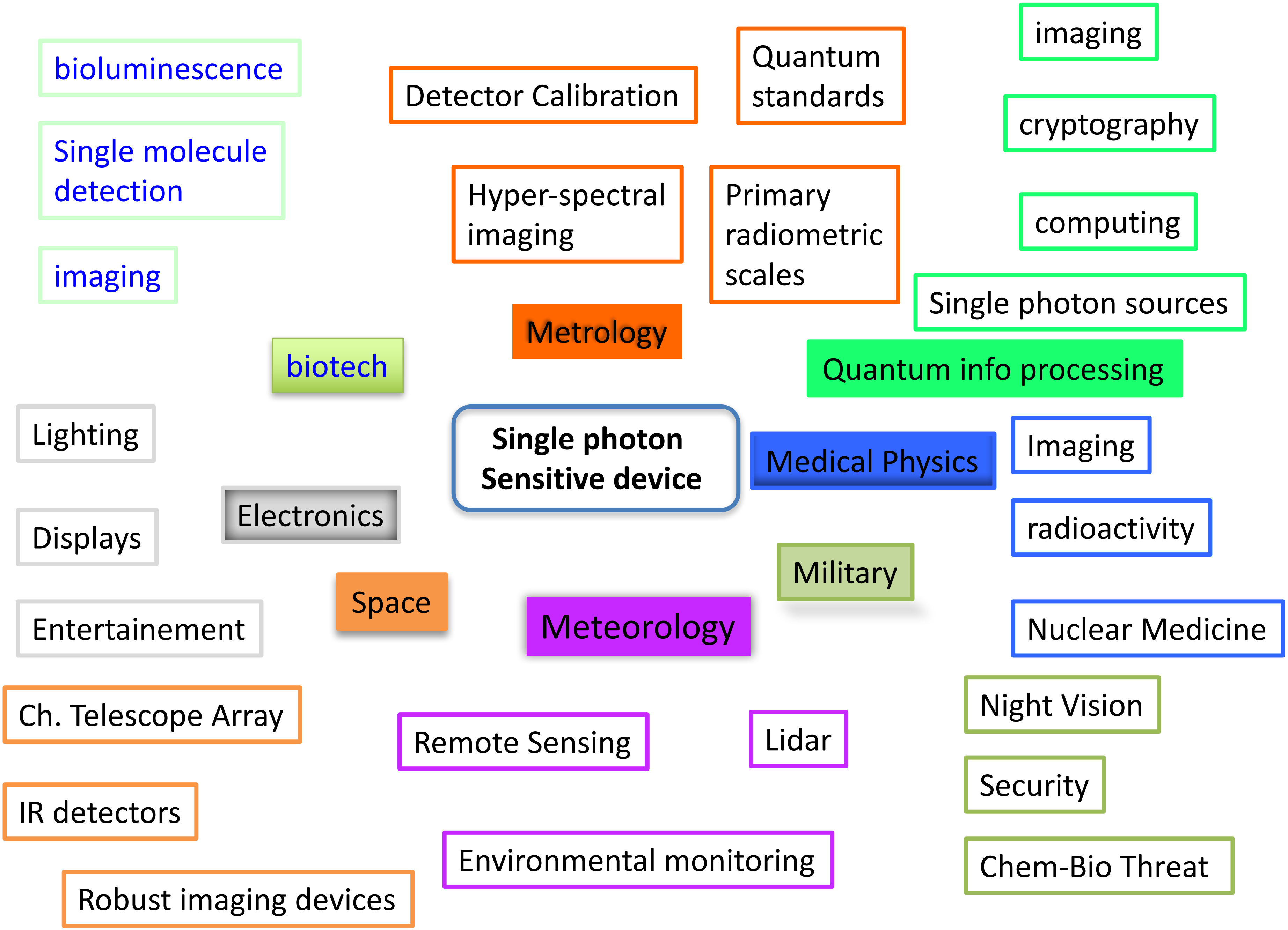

Summary Table from http://www.photoncount.org

A couple of futuristic applications that may intrigue you:

1. Quantum Technologies

Eur. Phys. J. D (2012) 66: 249
DOI: 10.1140/epjd/e2012-30351-6

THE EUROPEAN PHYSICAL JOURNAL D

Regular Article

Effect of the heralding detector properties on the conditional generation of single-photon states

V. D'Auria[1], O. Morin[2], C. Fabre[2], and J. Laurat[2,a]

[1] Laboratoire de Physique de la Matière Condensée, CNRS UMR 7336, Université de Nice-Sophia Antipolis, Parc Valrose, 06108 Nice Cedex 2, France
[2] Laboratoire Kastler Brossel, Université Pierre et Marie Curie, École Normale Supérieure, CNRS, Case 74, 4 place Jussieu, 75252 Paris Cedex 05, France

Received 4 June 2012
Published online 4 October 2012 – © EDP Sciences, Società Italiana di Fisica, Springer-Verlag 2012

Abstract. Single-photons play an important role in emerging quantum technologies and information processing. An efficient generation technique consists in preparing such states via a conditional measurement on photon-number correlated beams: the detection of a single-photon on one of the beam can herald the generation of a single-photon state on the other one. Such scheme strongly depends on the heralding detector properties, such as its quantum efficiency, noise or photon-number resolution ability. These parameters affect the preparation rate and the fidelity of the generated state. After reviewing the theoretical description of optical detectors and conditional measurements, and how both are here connected, we evaluate the effects of these properties and compare two kinds of devices, a conventional on/off detector and a two-channel detector with photon-number resolution ability.

Engineering single photon (deterministic!) sources and photon number resolving sensors is actually the name of the game in "quantum" technologies [cryptography, computing, networks]

nature COMMUNICATIONS

ARTICLE

Received 28 May 2013 | Accepted 10 Sep 2013 | Published 10 Oct 2013 DOI: 10.1038/ncomms3582 OPEN

Integrated spatial multiplexing of heralded single-photon sources

M.J. Collins[1], C. Xiong[1], I.H. Rey[2], T.D. Vo[1,3], J. He[1], S. Shahnia[1], C. Reardon[4], T.F. Krauss[2,4], M.J. Steel[5], A.S. Clark[1] & B.J. Eggleton[1]

The non-deterministic nature of photon sources is a key limitation for single-photon quantum processors. Spatial multiplexing overcomes this by enhancing the heralded single-photon yield without enhancing the output noise. Here the intrinsic statistical limit of an individual source is surpassed by spatially multiplexing two monolithic silicon-based correlated photon pair sources in the telecommunications band, demonstrating a 62.4% increase in the heralded single-photon output without an increase in unwanted multipair generation. We further demonstrate the scalability of this scheme by multiplexing photons generated in two waveguides pumped via an integrated coupler with a 63.1% increase in the heralded photon rate. This demonstration paves the way for a scalable architecture for multiplexing many photon sources in a compact integrated platform and achieving efficient two-photon interference, required at the core of optical quantum computing and quantum communication protocols.

The characterization of the statistics of photons emitted by a classical and quantum source is essential. This is requiring sensors with photon number resolving .

See also: M. Ramilli, M.C. et al, J. Opt. Soc. Am. B, Vol. 27, No. 5, May 2010

QuantumLeaps - March 2017

A couple of futuristic applications that may intrigue you:

2. Bio-applications

KUNGL.
VETENSKAPS-
AKADEMIEN
THE ROYAL SWEDISH ACADEMY OF SCIENCES

8 OCTOBER 2014

Scientific Background on the Nobel Prize in Chemistry 2014

SUPER-RESOLVED FLUORESCENCE MICROSCOPY

Awarded to: Eric Betzig, Stefan W. Hell, William E. Moerner

Heralded by Nature:

Method of the Year 2008

With its tremendous potential for understanding cellular biology now poised to become a reality, super-resolution fluorescence microscopy is our choice for Method of the Year.

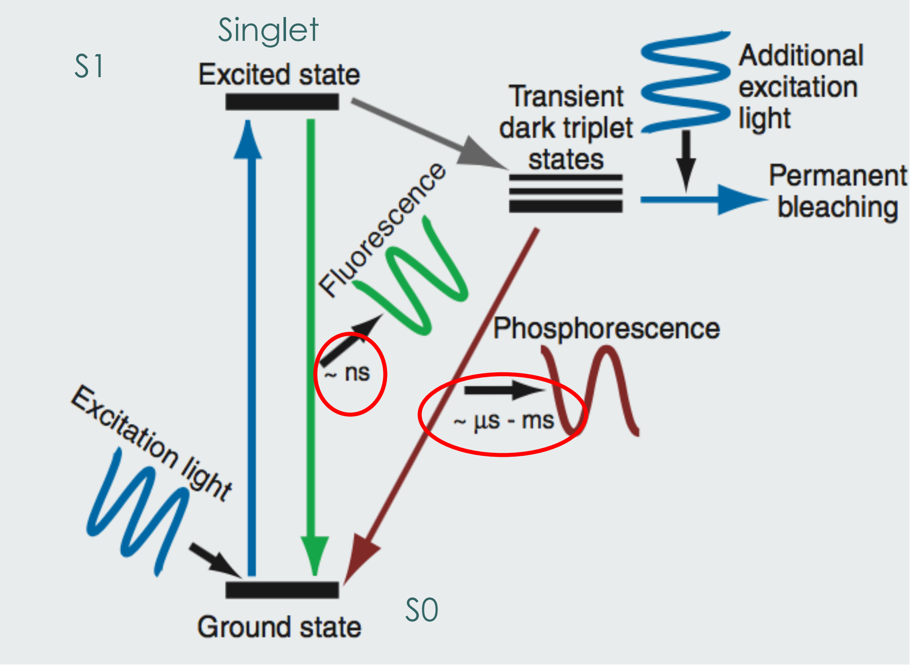

States and transitions of a fluorophore

Key issues:

- The lifetime of the emission from the Triplet state is O(10^6) wrt Singlet
- The transition probability to the Triplet state is O(0.1%)

⇒ with a continuous excitation of intensity 1kW/cm^2 the fraction of molecules in S0 << 10%

and for every cycle you will see a subset of molecules *blinking*

- Sub-diffraction limit imaging by stochastic optical recostruction microscopy (STORM)

Rust et al., Nature Methods vol.3 NO.10 | OCTOBER 2006 | **793**

- Fluorescence Nanoscopy by ground state depletion and single molecule return (GDSIM)

Folling et al., Nature Methods vol.5 NO.11 | OCTOBER 2008 | 943

Heralded by Nature:

Method of the Year 2008

With its tremendous potential for understanding cellular biology now poised to become a reality, super-resolution fluorescence microscopy is our choice for Method of the Year.

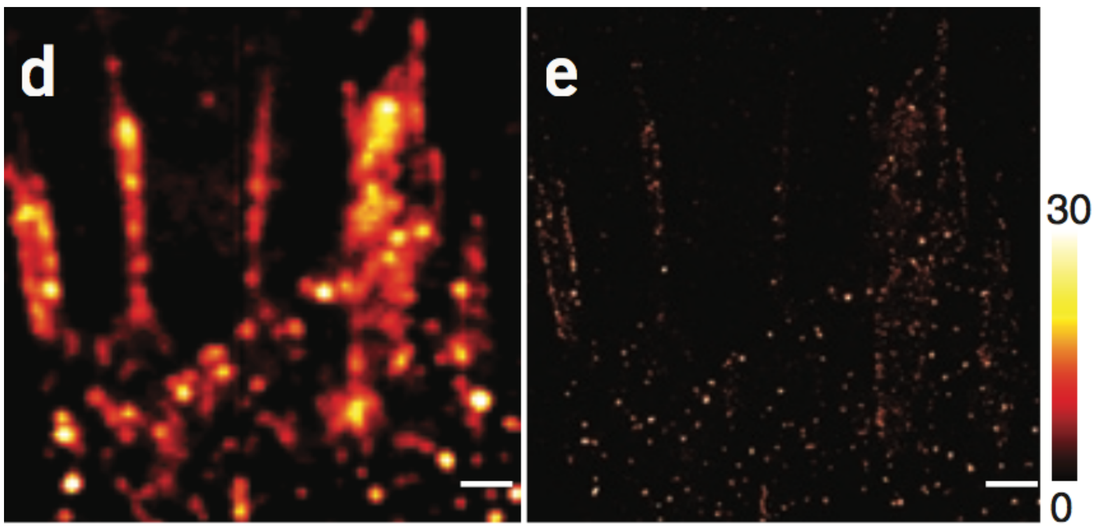

- Camera frame: 200 Hz
- No. frames: 31 000
- Laser intensity: 2.5 kW/cm^2
- Laser wavelength: 532 nm

Immunostained (Atto532) integrin-β-3 clusters of human glioma cells in a cell medium

- Fluorescence Nanoscopy by Ground State Depletion and Single Molecule return (GDSIM)

Folling et al., Nature Methods vol.5 NO.11 | OCTOBER 2008 | 943

Heralded by Nature:

Method of the Year 2008

With its tremendous potential for understanding cellular biology now poised to become a reality, super-resolution fluorescence microscopy is our choice for Method of the Year.

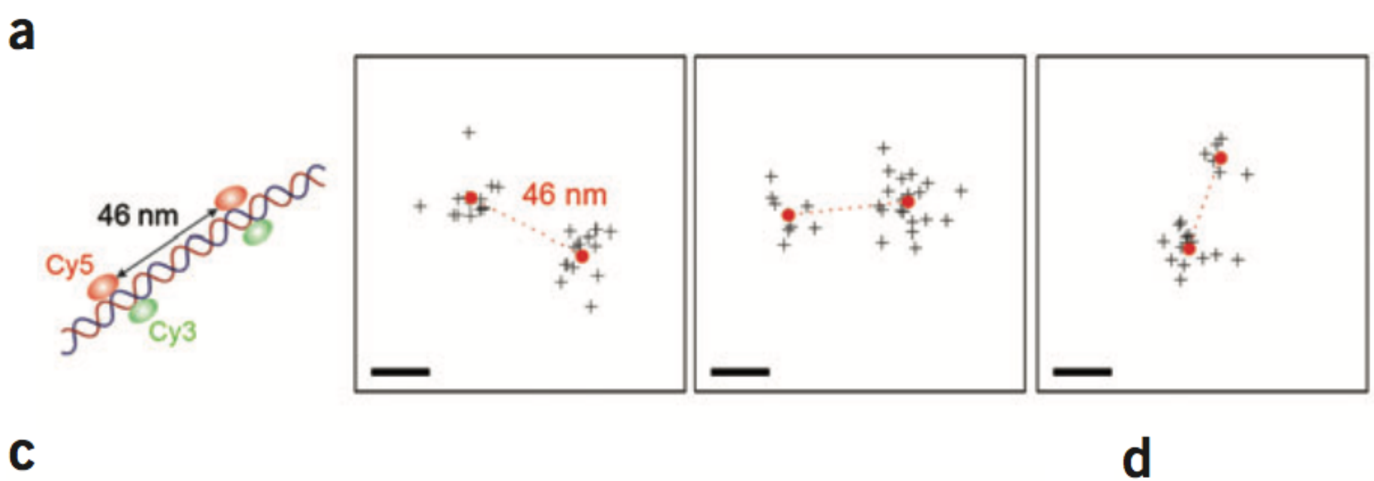

Separation between "switches" attached to a DNA molecule separated by a well known number of base pairs

- Sub-diffraction limit imaging by STochastic Optical Recostruction Microscopy (STORM)

Rust et al., Nature Methods vol.3 NO.10 | OCTOBER 2006 | **793**

How can we get there?
[step 2]

Do for light what you do with sound:
Pump up the volume of the light!

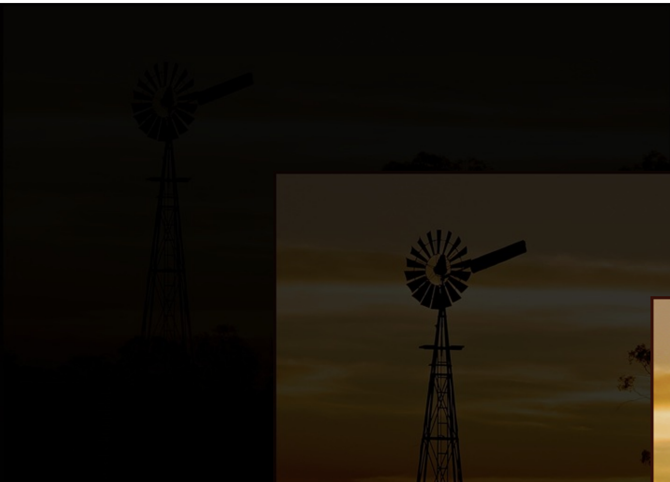

1/4

1/2

1

3/2

7/4

Get every single light droplet and
transform it into a heavy shower!

The pre-Silicon age:

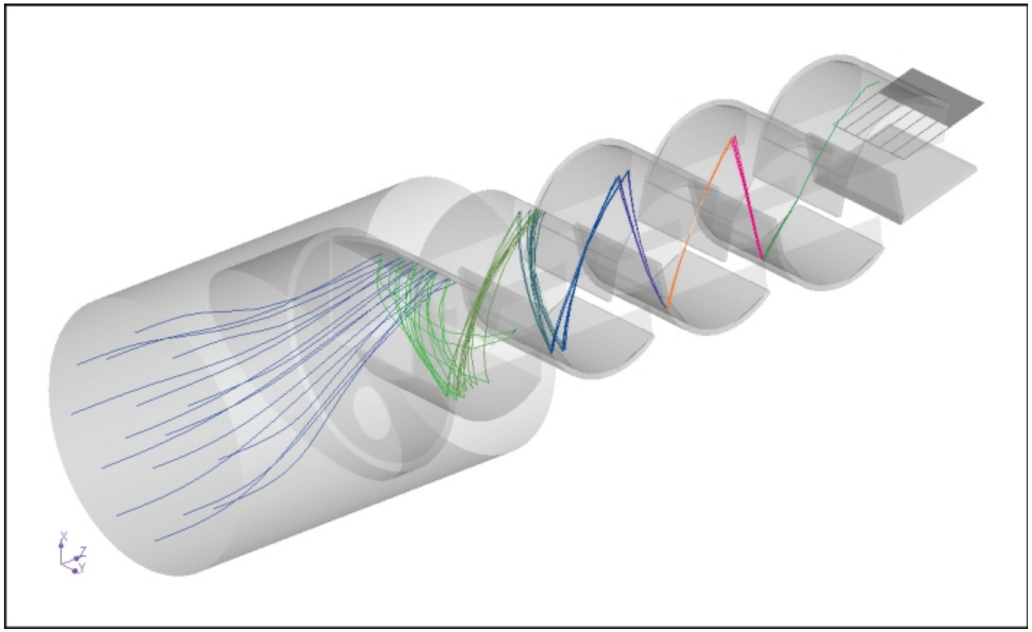

the photomultiplier (PMT), a solid rock technology since 1934

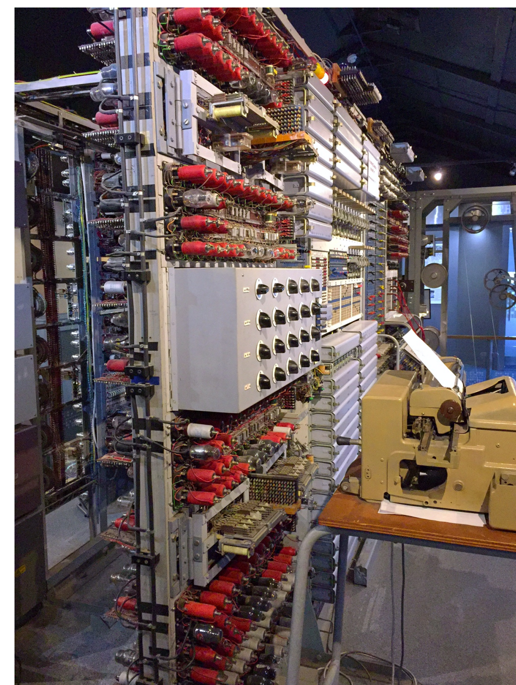

PMT somehow reminds Thermoionic Valves

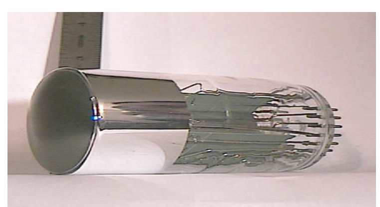

The Colossus (1944), containing on 1700 thermoionic valves

What happened when Silicon entered the game?

The first point contact transistor
William Shockley, John Bardeen, and Walter Brattain
Bell Laboratories, Murray Hill, New Jersey (1947)

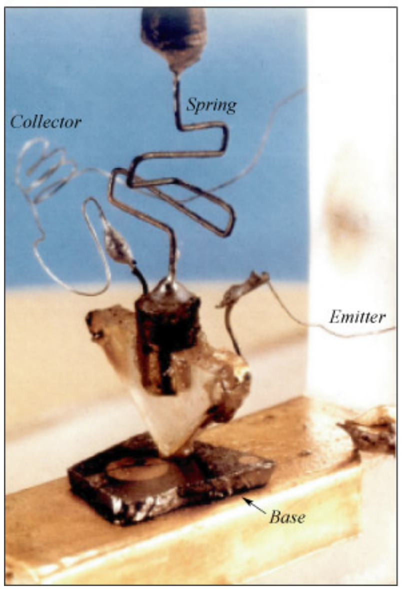

You do not need ME to tell YOU....

The Silicon age in Photonics: photon absorption and avalanche ignition in a Single Photon Avalanche Photodiode (SPAD)

A pioneering development by Prof. S. Cova
at Politecnico di Milano

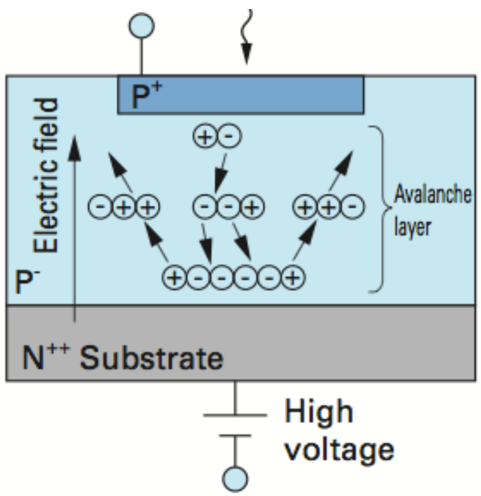

- Very shallow p-n junction
  ➔ ~ 1 μm
- High electric field
  ➔ > 3 x 10^5 V/cm
- Mean free path
  ≈ 0.01 μm

When a photon hits a cell, the generated charge carrier triggers an avalanche multiplication in the junction by impact ionization, with gain at the 10^6 level

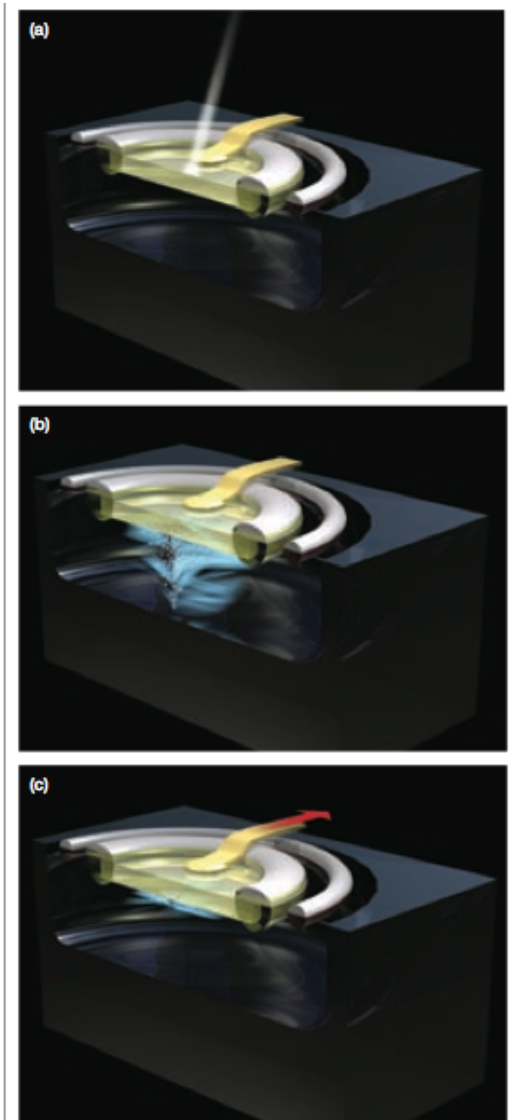

[an artist's view]

E. Charbon & S. Donati, OPN Optics & Photonics News, February 2010

A multiplication game in Silico
[courtesy of Ivan Rech, Politecnico di Milano]

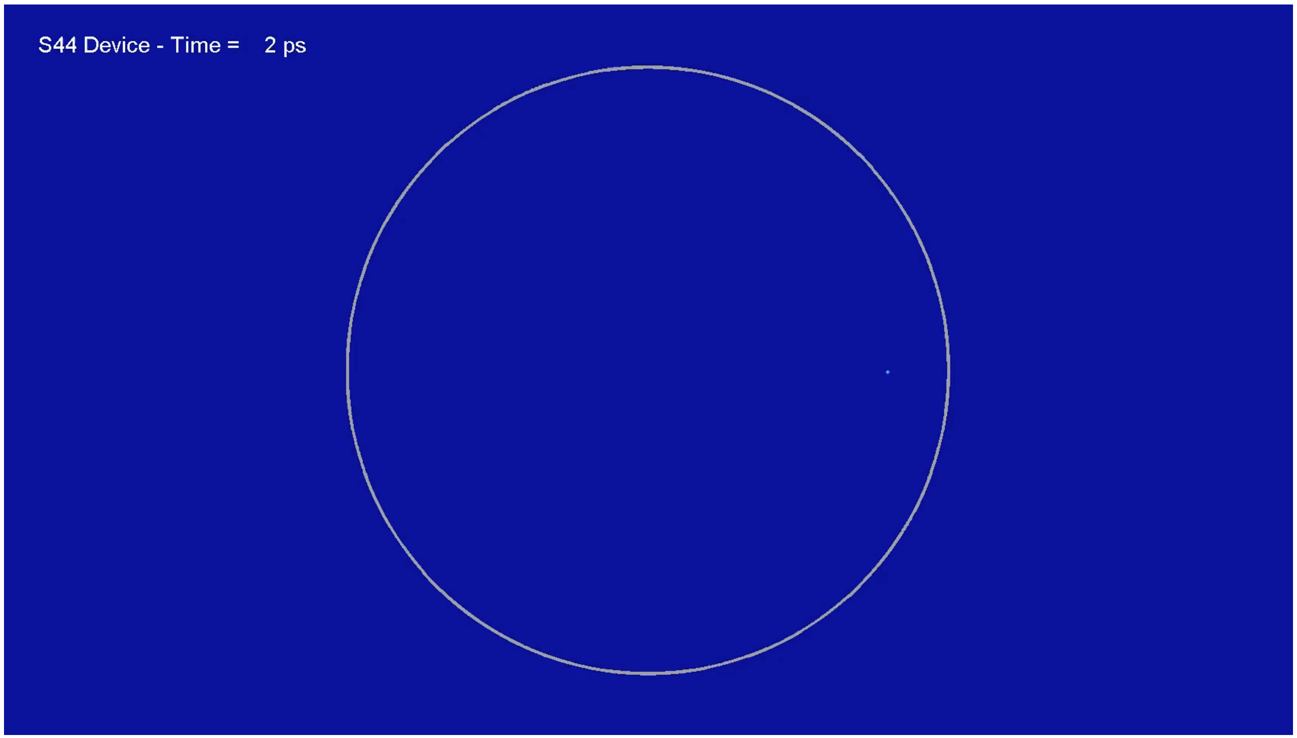

- Spread of the avalanche essentially diffusion assisted (with minor contributions from photons)
- Speed 10-20 μm/ns (this cell has a diameter of 50 μm)

Essentially a binary cell, turning from black to white when a photon is detected – the building block of our sensor

1. A. Gulinatti , I. Rech , M. Assanelli , M. Ghioni & S. Cova (2011) A physically based model for evaluating the photon detection efficiency and the temporal response of SPAD detectors, Journal of Modern Optics, 58:3-4, 210-224, DOI: 10.1080/09500340.2010.536590
2. A. Gulinatti, I. rech et al., Modeling photon detection efficiency and temporal response of single photon avalanche diodes , Proc. of SPIE Vol. 7355 73550X-1
3. Spinelli, A. and Lacaita, A. L. "Physics and numerical simulation of single photon avalanche diodes", IEEE Transactions on Electron Devices, 44(11), 1931—1943 (1997).

*S*ilicon Photomultipliers:
fundamentals & main features,
pros & cons

[step 3]

Silicon Photon Multipliers (SiPM):
genuine *Photon Number Resolving Detectors*

SiPM = High density ($\sim 10^4/mm^2$) matrix of diodes with a common output, reverse biased, working in Geiger-Müller regime, essentially an array of SPAD

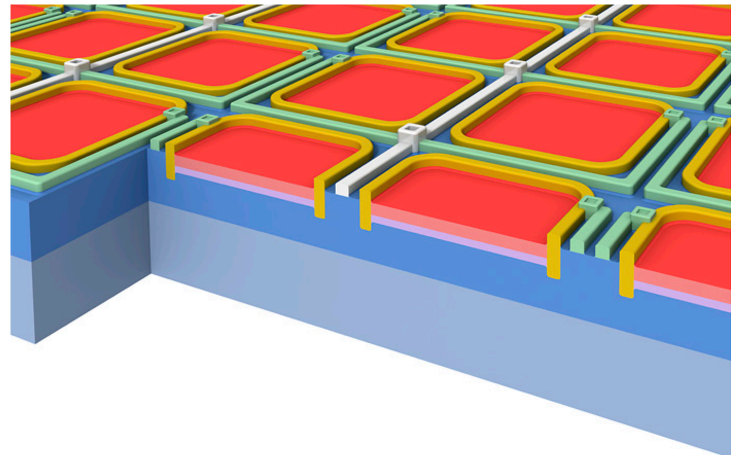

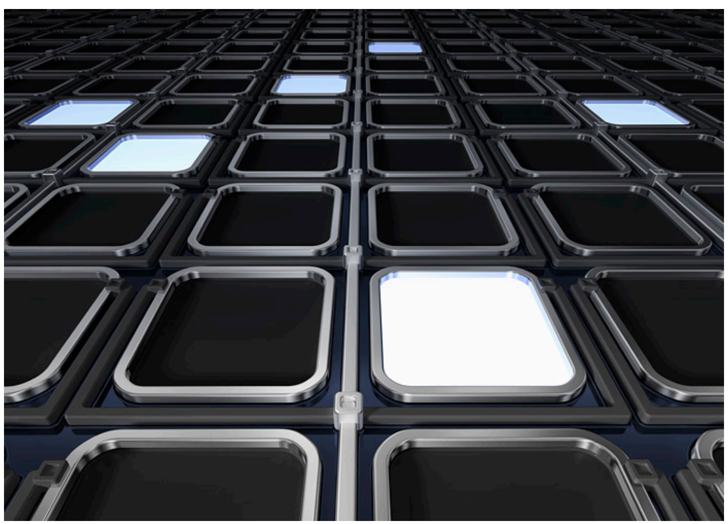

❖ SiPM may be seen as a collection of binary cells, fired when a photon in absorbed

❖ "counting" cells provides an information about the intensity of the incoming light

Courtesy http://www.yk.rim.or.jp/~reyhori/pages/galacc2_e.html

Silicon Photon Multipliers (SiPM):
genuine *Photon Number Resolving Detectors*

SiPM = High density (~10^4/mm^2) matrix of diodes with a common output, reverse biased, working in Geiger-Müller regime, essentially an array of SPAD

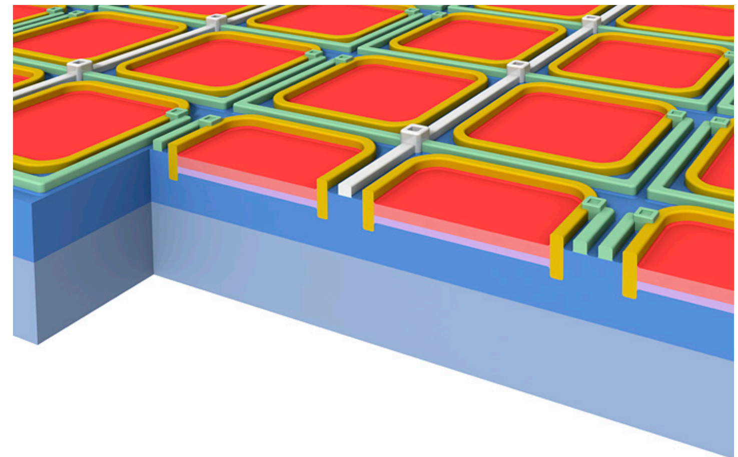

Courtesy http://www.yk.rim.or.jp/~reyhori/pages/galacc2_e.html

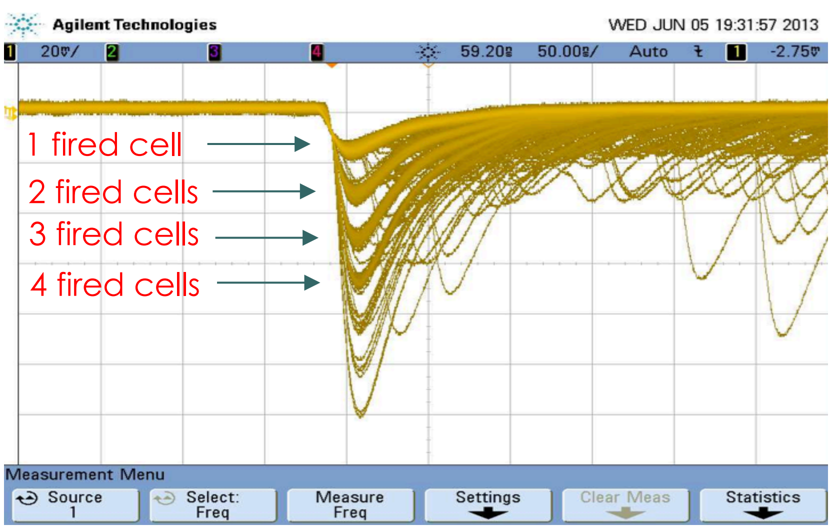

Counting is possible at the oscilloscope!

Response of a SiPM to a plurality of low light pulses, where the full information is conveyed by the signal area

Silicon Photon Multipliers (SiPM):

genuine *Photon Number Resolving Detectors*

A histogram of a large statistics of integrated signals in response to a fast pulse of light can teach you a lot, both in terms of the emitted photon statistics and of the detector itself:

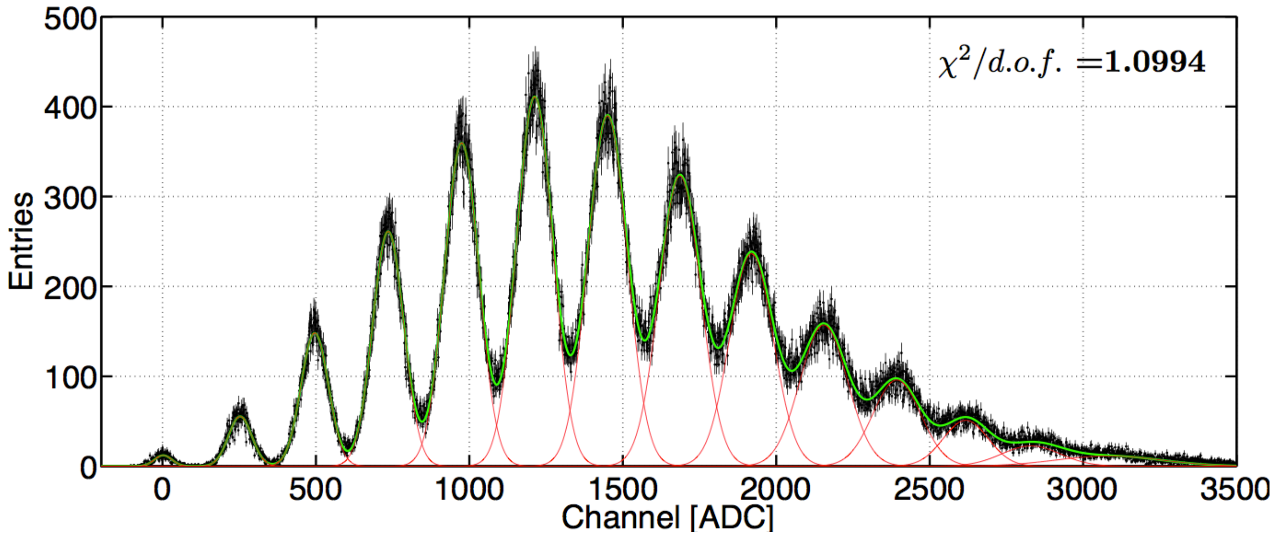

- *On the characterisation of SiPMs from pulse-height spectra, V. Chmill, E. Garutti, R. Klanner, M. Nitschke, J. Schwandt, 10.1016/j.nima.2017.02.049*
- *A robust and semi-automatic procedure for Silicon Photomultipliers characterisation, V. Arosio, M. Beretta, M. Cacciaa and R. Santoro – 2017 JINST 12 C03030*
- *Reconstruction of the statistics of photons by a pulsed LED using a Silicon Photomultiplier based set-up , V. Arosio et al. – 2015 JINST 10 C08008*

SiPM: simplified electrical model

- Roland Heitz, Journal of Applied Physics **35**, 1370 (1964)
– C. Piemonte, NIM A 568 (2006) 224–232
– S. Seifert et al., IEEE TRANSACTIONS ON NUCLEAR SCIENCE, VOL. 56, NO. 6, 2009
– P. Hallen, bachelor thesis, Aachen University, 2011
– F.Licciulli, C.Marzocca, IEEE TRANSACTIONS ON NUCLEAR SCIENCE, VOL. 63, NO. 5, 2016
– Chen Xu, Robert Klanner, Erika Garutti, Wolf-Lukas Hellweg, Nucl.Instrum.Meth. A762 (2014) 149-161

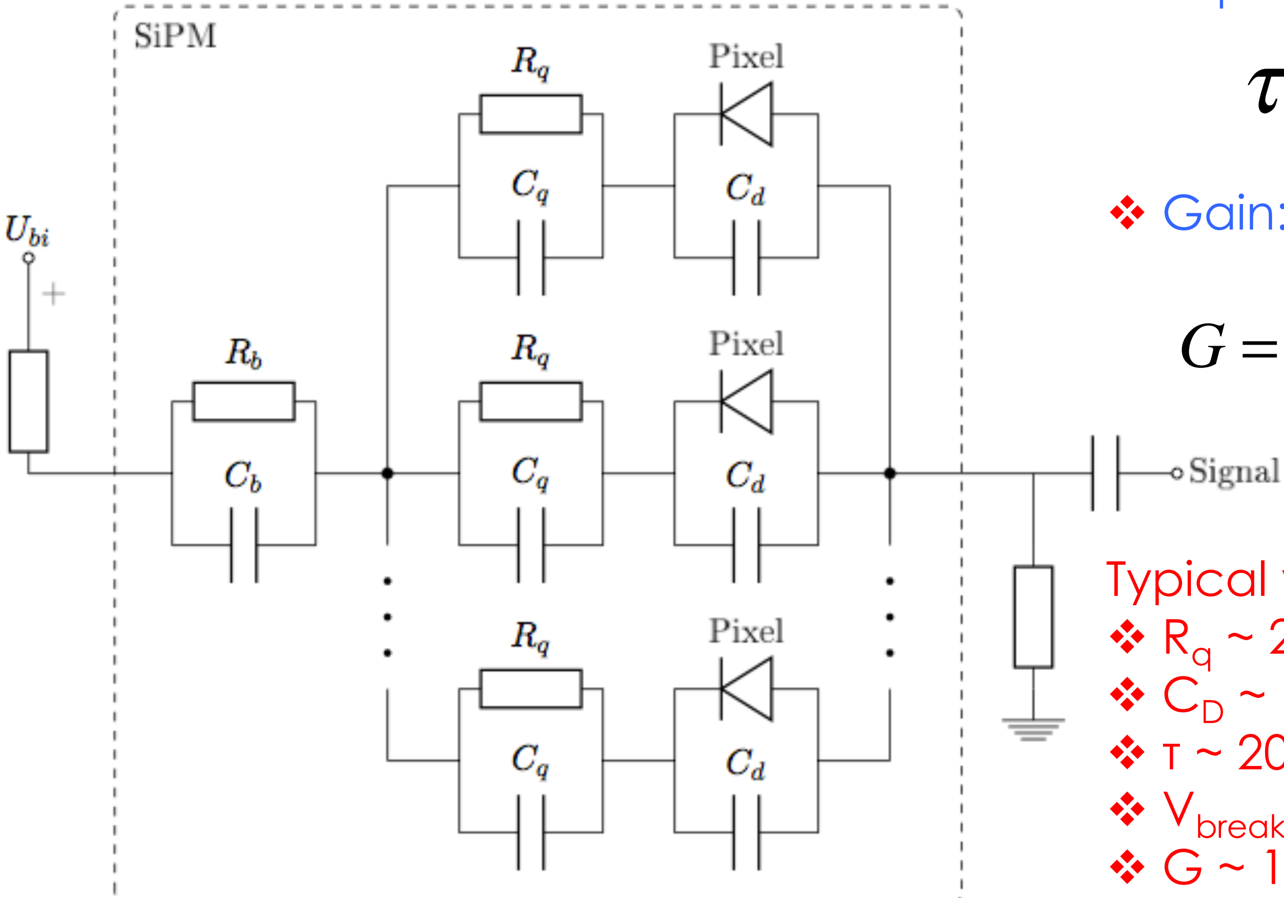

- exponential recharge with

$$\tau = R_q C_D$$

- Gain:

$$G = \frac{(V_{bias} - V_{Breakdown})C_D}{e}$$

Typical values:

- R_q ~ 200 kΩ
- C_D ~ 100 fF (30x30 μm^2)
- τ ~ 20 ns
- $V_{breakdown}$ ~ 50-70V
- G ~ 10^6

NB: references provided to go beyond the simplified model

Is the world interested in these little toys?

No. of papers in Google Scholar with the exact match of "silicon photomultiplier" in the title/abstract/body

Year	# papers
2000-2001	13
2002-2003	40
2004-2005	155
2006-2007	430
2008-2009	745
2010-2011	1334
2012-2103	2430
2014-2015	2720
2016-Sep2017	2480

SiPM are available by different producers (e.g. HAMAMATSU, SensL, KETEK) in a large variety of cell size and area, impacting on their key parameters.

The optimal choice is application dependent.

In terms of pixel pitch:

$10\ \mu m$

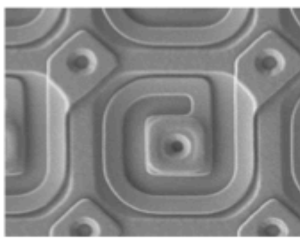

$15\ \mu m$

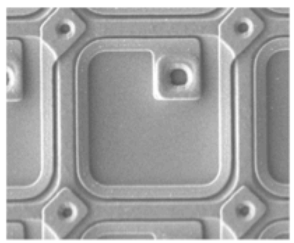

$25\ \mu m$

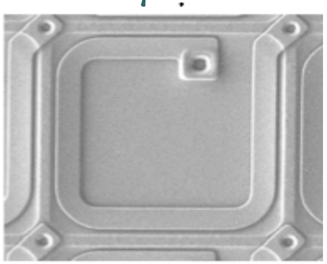

$50\ \mu m$

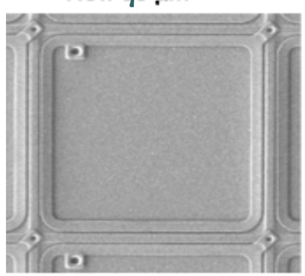

75 & 100 μm *are available as well*

In terms of sensitive area:

- 1x1 mm^2
- 3x3 mm^2
- 6x6 mm^2

- 1x4 mm^2
- 12x12 mm^2
- 24x24 mm^2

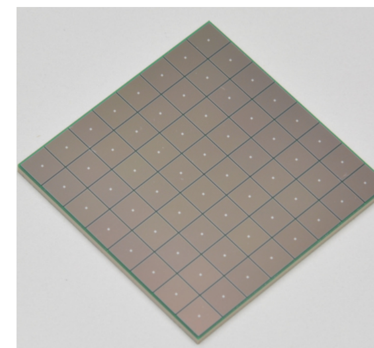

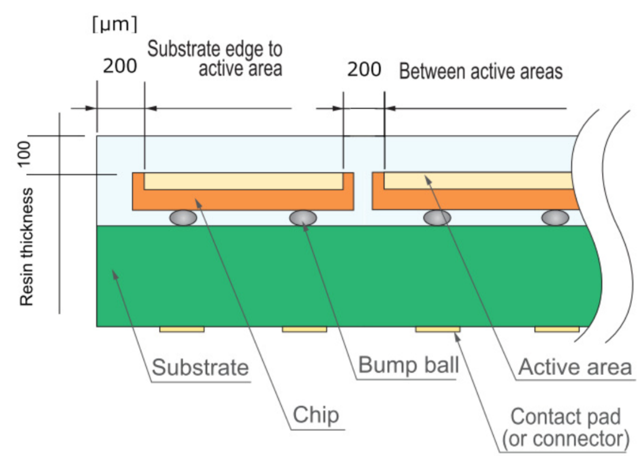

The main sensor parameters

- Photon Detection Efficiency, spectral response & linearity

- Stochastic terms:
  - Darks counts
  - Optical cross talk
  - Afterpulsing

  [cell-to-cell gain variation neglected]

- Gain & its stabilization

Photon detection efficiency (PDE), namely the ratio between the number of incoming photons and the number of fired cells (or photo-electrons (p.e.) triggering an avalanche)

$$n_{p.e.} = n_{photons} \times [QE][FillFactor][P_{GM}]$$

Essentially a technology parameter: it measures the fraction of the area sensitive to light (i.e. not covered by metal lines, poly-resistors, trenches, else)

Pitch = 10 μm

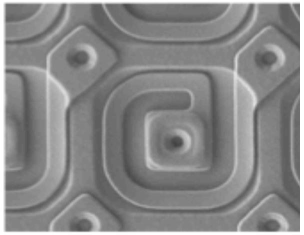

Pitch > 50 μm

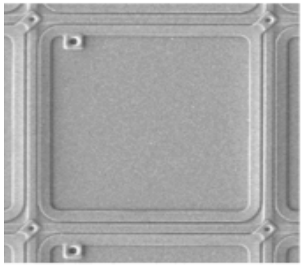

The larger the pitch, the higher the Fill Factor

Photon detection efficiency (PDE), namely the ratio between the number of incoming photons and the number of fired cells (or photo-electrons (p.e.) triggering an avalanche

$$n_{p.e.} = n_{photons} \times [QE][FillFactor][P_{GM}]$$

Essentially Physics driven: it measures the probability that a charge carrier initiates an avalanche

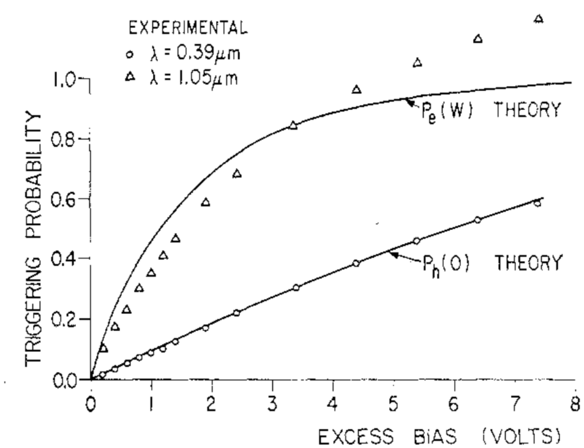

The higher the Excess Bias (over-voltage) the better it is since the ionization coefficients increase with the electric field:

$$\alpha = a \times e^{\frac{-b}{E}}$$

where $a \approx 10^6$, $b \approx 2\text{x}10^6$

Oldham et al, IEEE 'TRANSACTIONS ON ELECTRON DEVICES, **VOL.**ED-19, NO. 9,SEPTEMBER 1972

Photon detection efficiency (PDE), namely the ratio between the number of incoming photons and the number of fired cells (or photo-electrons (p.e.) triggering an avalanche

$$n_{p.e.} = n_{photons} \times [QE][FillFactor][P_{GM}]$$

Related to the material properties and the junction technology:

Blue (470nm)	0.6 μm
Green (525nm)	1.2 μm
Yellow (590nm)	2.2 μm
Red (625nm)	2.9 μm

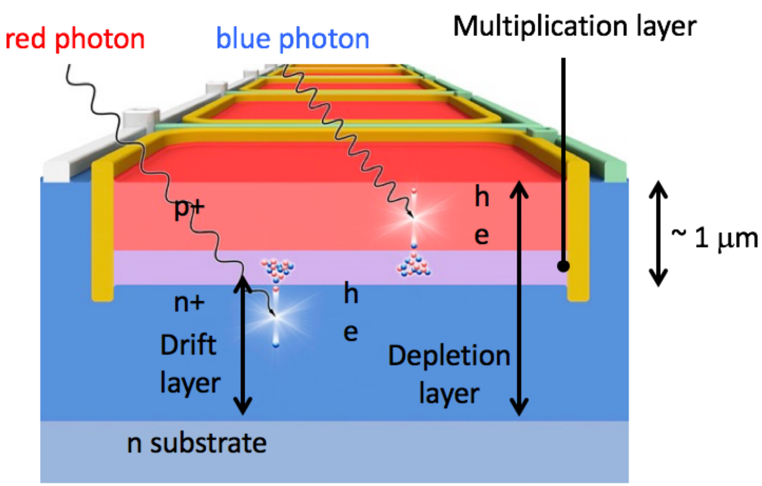

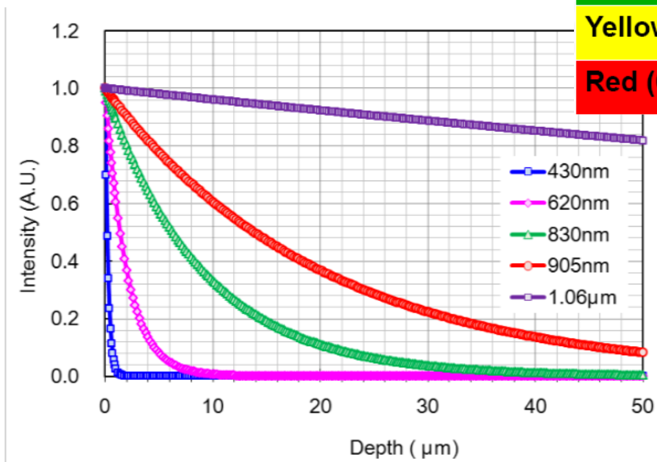

Light attenuation vs depth [μm]

Photon detection efficiency (PDE), namely the ratio between the number of incoming photons and the number of fired cells (or photo-electrons (p.e.) triggering an avalanche

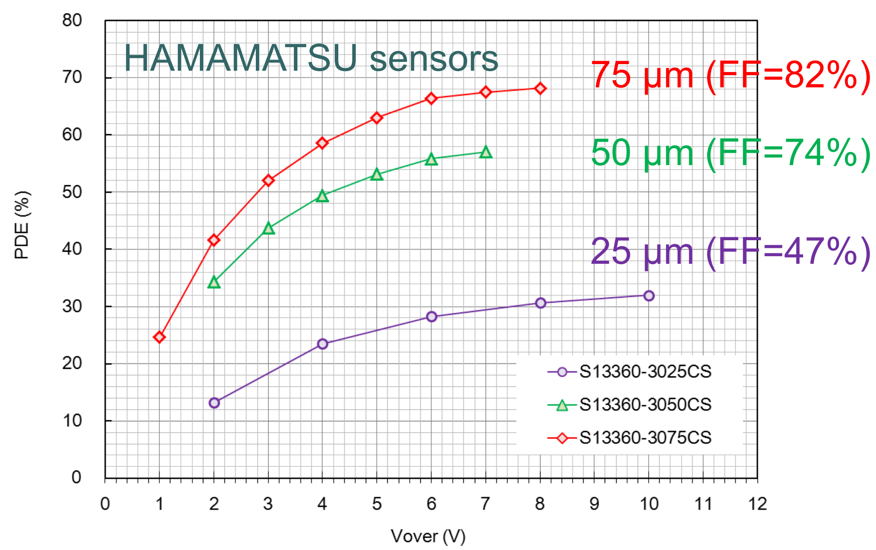

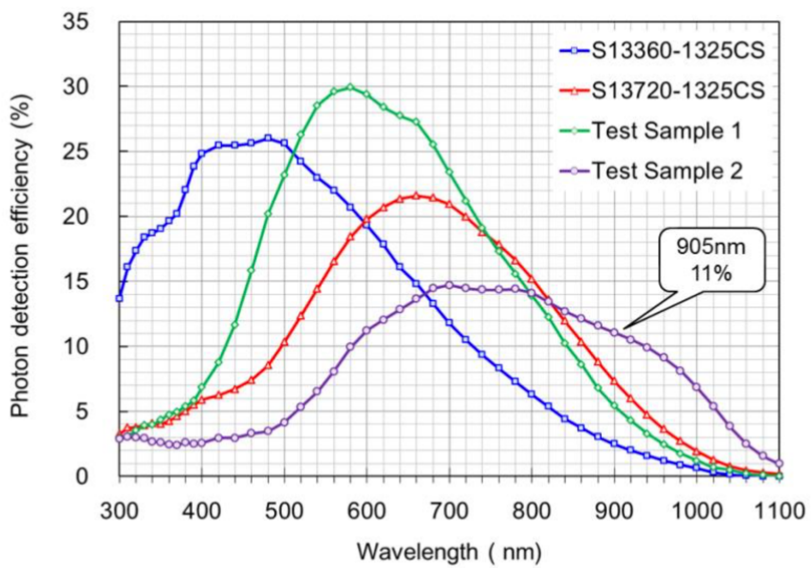

Spectral response

Fill factor

	S13360 Series
75 µm	82%
50 µm	74%
25 µm	47%

K.E. Kuper et al. 2017 *JINST* **12** P01001

Non-linearity in the response due to photons occasionally hitting the same cell

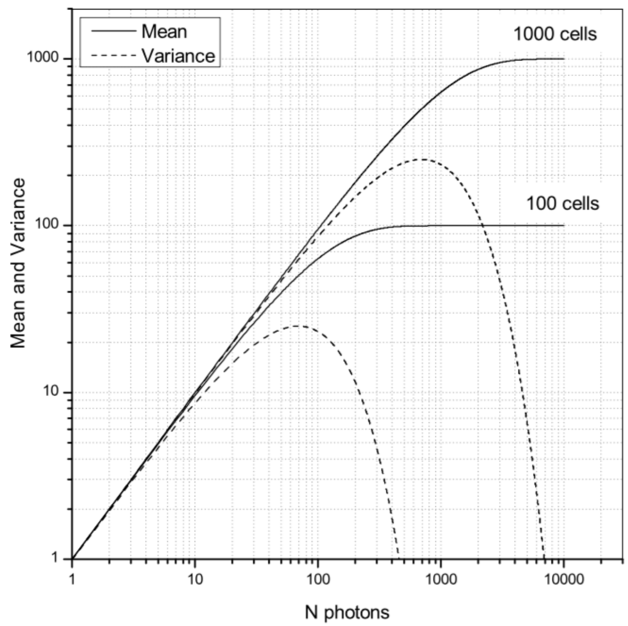

How do I get to this magic formula? In essence, it is a problem related to the finite number of cells & Geiger-Mueller process: as long as the probability of having more than one photo-electron (i.e. photon induced avalanche) in a single cell is not negligible, I can expect a deviation from the linearity in the response.

$$N_{fired} = N_{cells} \times \left[1 - e^{\frac{-N_{photons} \times PDE}{N_{cells}}}\right]$$

About balls & baskets [see also Stoykov et al., 2007 JINST 2 P06005]

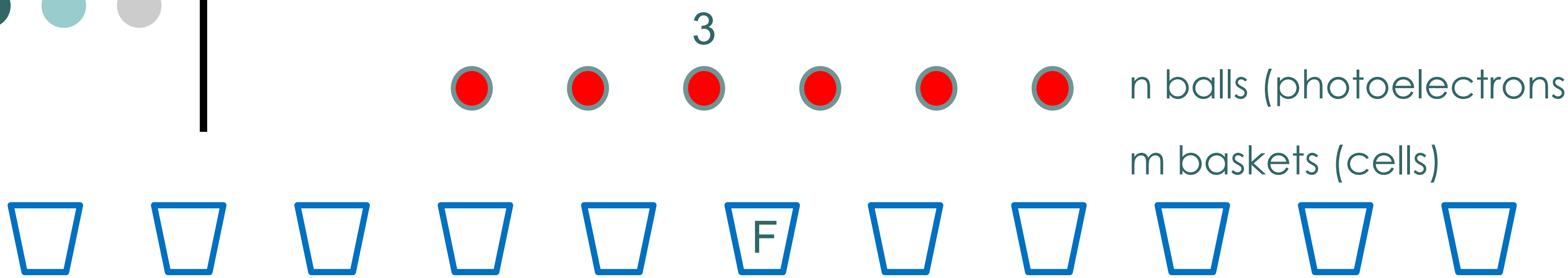

Presume that the balls are randomly thrown into the baskets. Then:

- The probability of a ball (say 3) to get into a specific basket (say F) is $1/m = m^{-1}$

  $\Longrightarrow$ The probability of NOT being hit is $(1- m^{-1})$

  $\Longrightarrow$ The probability that NONE of the n balls enters F is $(1- m^{-1})^{n}$ (assuming the events to be uncorrelated)

  $\Longrightarrow$ The probability to have ONE OR MORE balls in F is $p=(1-(1- m^{-1})^{n}))$

- But F is like any other basket $\Rightarrow$ I can turn the problem in the same category of the "coin toss" statistics (Bernoullian or Binomial), where the coin is not a fair coin but the probability to get "head" is p:

$\Longrightarrow$ The mean number of baskets having at least one ball is $\bar{N} = m \times p$

$\Longrightarrow$ The standard deviation in the number of cells having at least one ball is

$$\sigma = \sqrt{m \times p \times (1-p)}$$

As long as the number of baskets (cells) is large:

$$1 - m^{-1} \simeq e^{-\frac{1}{m}}$$

$$p \simeq 1 - e^{-\frac{n}{m}} = 1 - e^{-\frac{N_{photons} \times PDE}{N_{cells}}}$$

And I get the magic formula (together with the fact that the standard deviation in the response, i.e. the fluctuations, do increase since the response is affected by the randomness of the detection process)

Dark Count Rate (DCR)

It measures the rate at which a Geiger avalanche is randomly initiated by thermal emission or tunneling

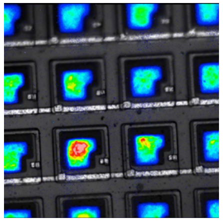

❖ DCR today: ~ 100 kHz/mm^2 with the possibility to reduce it considerably by cooling:

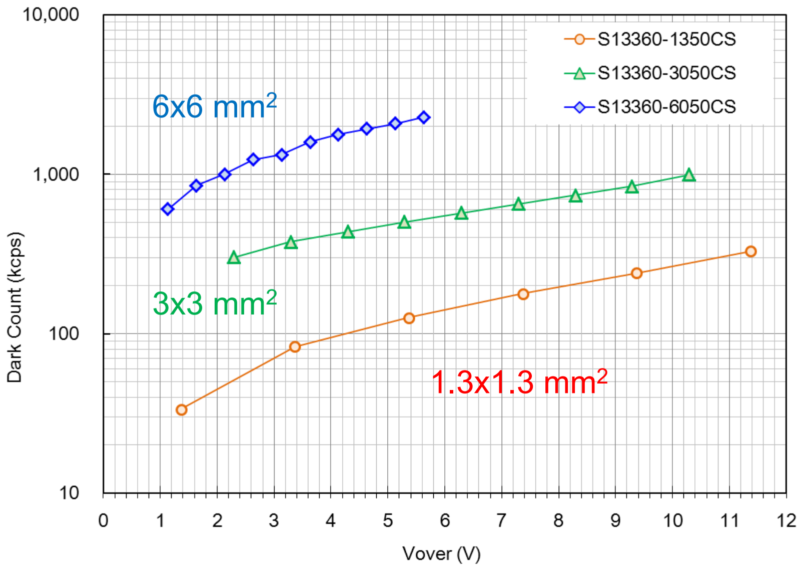

Exemplary figures for sensors with 50 μm pitch

	Dark Count Vover = 3 V
1.3x1.3 mm	90 kcps
3x3 mm	500 kcps
6x6 mm	2 M cps

N.B. The dark count decreases by half for every approx. 8 °C drop in temperature

Optical Cross Talk (OCT) *(A. Lacaita et al, IEEE TED (1993))*

It measures the rate at which photons generated during the Geiger avalanche fire a neighbouring pixel → Spurious pulses are not limited to the single cell amplitude!

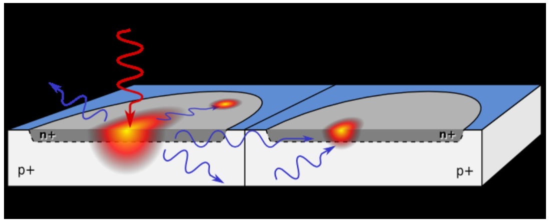

- during Geiger avalanche ~3 emitted γ / 10^5 carriers with E_γ > 1.14 eV
- absorption coefficient ~2μm

❖ OCT today:

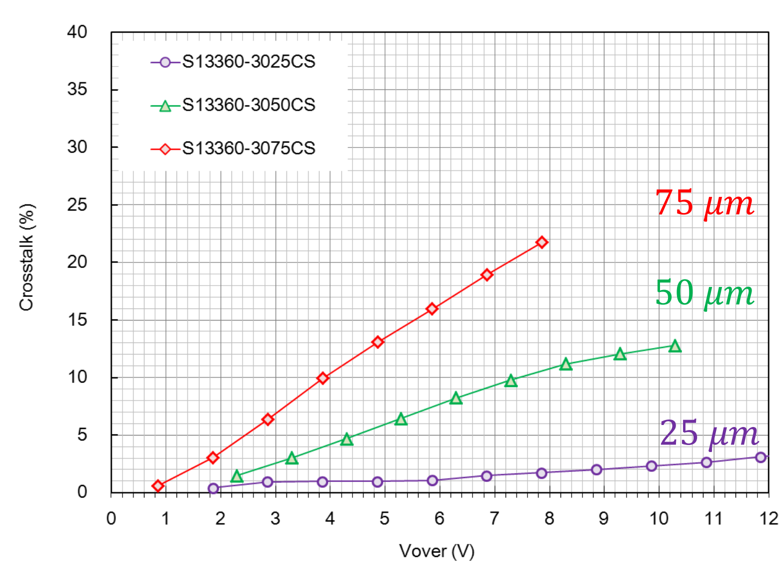

	Crosstalk Vover = 3 V	Gain
25 µm	1 %	7.0×10^5
50 µm	3 %	1.7×10^6
75 µm	7 %	4.0×10^6

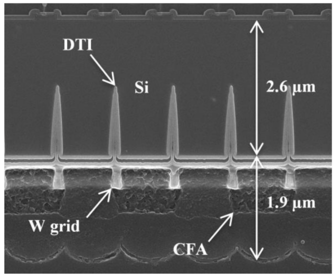

Samsung S5K2P2XX (partial) DTI

Trench isolation, mutuated from the imaging technology

Larger pixels have a higher gain ➔ higher probability to have a secondary photon to trigger a neighbouring cell

After-pulsing

Delayed avalanches triggered by the release of a charge carriers that has been produced in the original avalanche and trapped on an impurity; the release of the trapped carriers is characterizated by a typical decay time ~200 ns

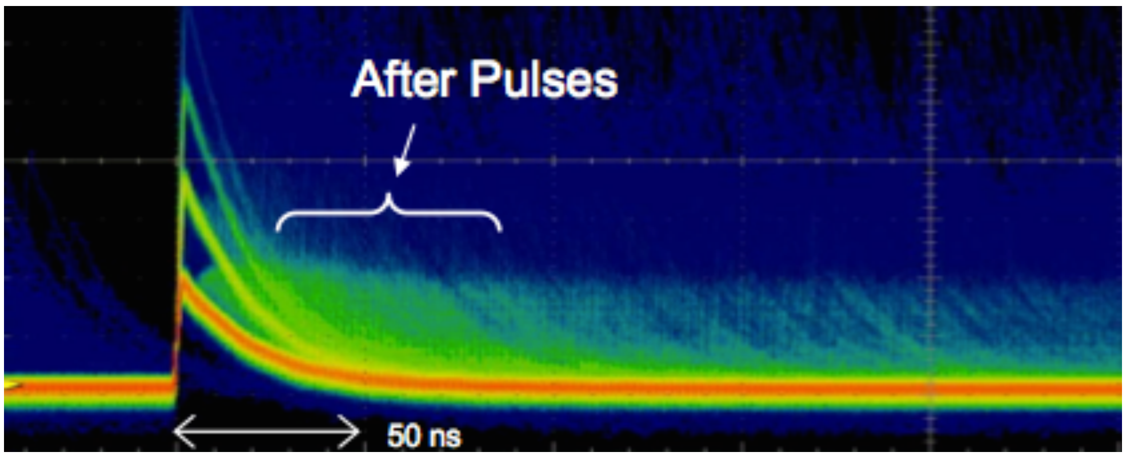

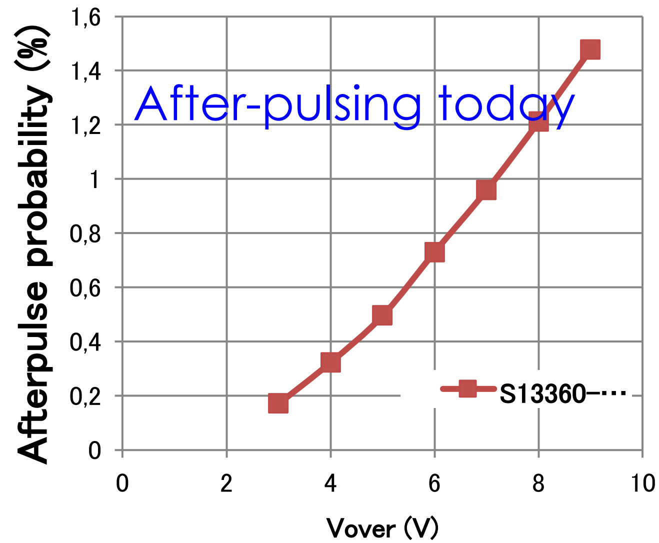

- Y. Du, F. Retiere (NIM A 596 (2008) 396–401
- Eckert et al., arXiv:1003.6071v2 (2010)
- M. Caccia et al., JIINST 9 T10004 (2014)

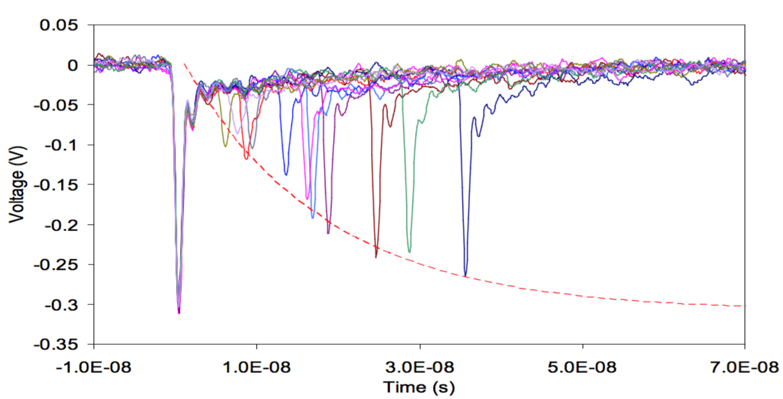

The amplitude of the after-pulse signals depends on the recovery stage of the pixel

C. Piemonte, IEEE TRANSACTIONS ON NUCLEAR SCIENCE, VOL. 54, NO. 1, 2007

Temperature dependence of the gain & its stabilization

- C.R. Crowell, S.M.Sze, "TEMPERATURE DEPENDENCE OF IN SEMICONDUCTORS", APPLIED PHYSICS LETTERS 9, pag. 242, 1966
- C. Y. Chang, S. S. Chiu, and L. P. Hsu, "Temperature dependence of breakdown voltage in silicon abrupt P-N junctions," IEEE Trans. Elec- tron Devices, vol. 18, no. 6, pp. 391–393, 1971

Unfortunately, the interaction with phonons (vibrational quanta) has an impact on the energy of charge carriers, their ionization coefficients and eventually their breakdown voltage. Since phonons spectra & mean free path have a temperature dependence, so does the breakdown voltage:

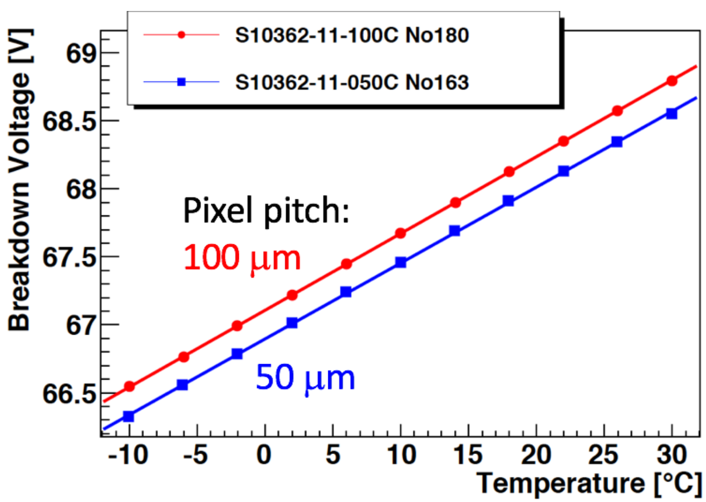

A. Taddey, Terascale Workshop, UniHamburg

$$V_{Br}(T) = V_{Br}(T_o) \times [1 + \beta(T - T_o)]$$

22 mV/^{o}K < β < 55 mV/^{o}K

Unless you stabilize the temperature OR the biasing voltage in terms of Excess Bias, the detector gain will drift with T

A fairly good example (historically relevant)

M. Ramilli, "Characterization of SiPM: Temperature dependencies," in Proc. 2008 IEEE Nucl. Sci. Symp. Med. Imag. Conf. Rec., 2008, pp. 2467–2470.

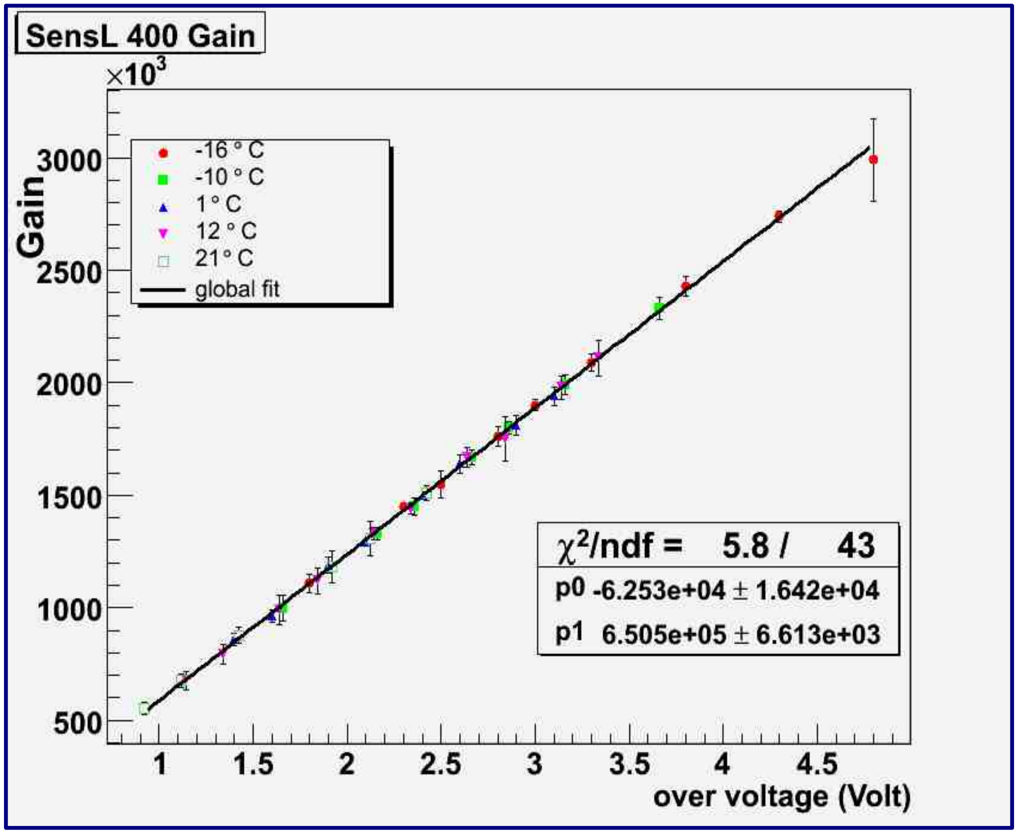

- T was measured as close as possible to the sensor
- The biasing voltage was tuned to keep the Excess Bias constant

What's next?

Trends in the R&D (user's driven, steered by the companies):

- Make it (more) quiet (decrease the stochastic terms)

+

= Noise Reduction Rating of 34

NRR 29

NRR 27

Trends in the R&D (user's driven, steered by the companies):

- Increase the cell densities (extend the dynamic range)

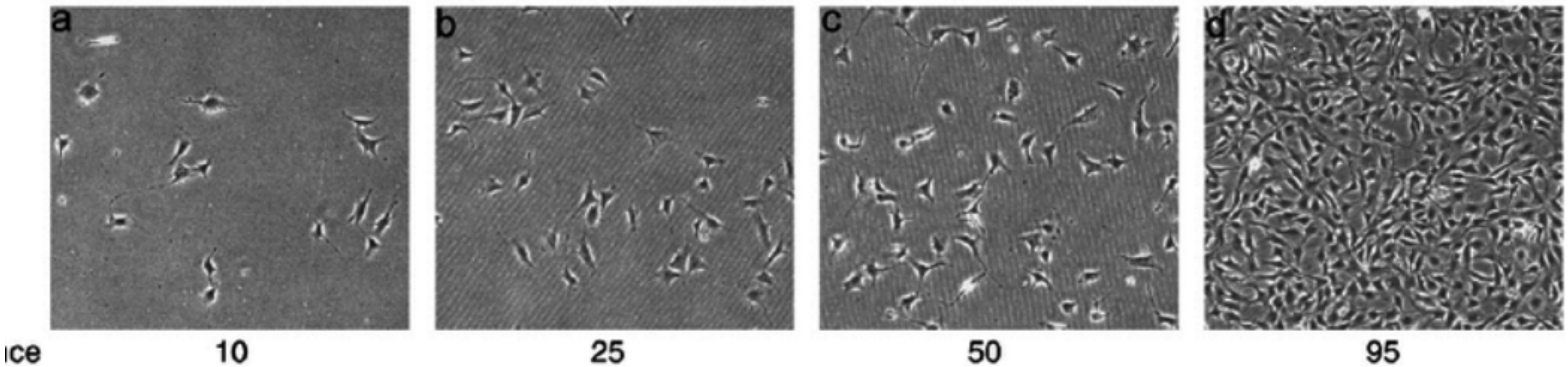

Trends in the R&D (user's driven, steered by the companies):

- Push the sensitivity a bit to the right (NIR)

- … and to the left (NUV)

Trends in the R&D (user's driven, steered by the companies):

- Integrate a bit of intelligence on board

Trends in the R&D (user's driven, steered by the companies):

- Look at the NewKidsOnTheBlock

Broadcom succesfully negotiated an exclusive license of the NUV-HD technology from FBK:

Broadcom is aiming to:
- high-volume production;
- Wafer-level packaging with TSVs.

Parameter	Value
PDE (%)	55
DCR @ 20 C (kcps)	55
Optical cross-talk (%)	9
After-pulsing (%)	<1
Breakdown voltage, V_{BD} (V)	27
V_{BD} temperature coefficient (mV/C)	25

30 µm cell pitch

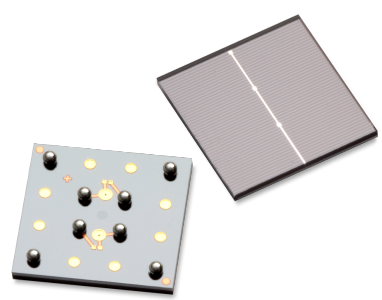

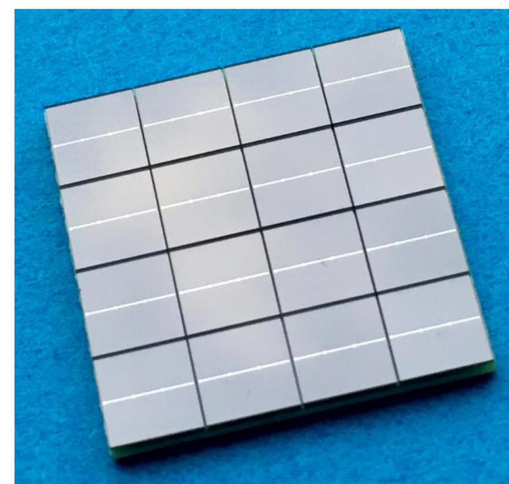

SiPM for Time of Flight LIDAR: the latest from SensL

The basic principle

Challenges:

- Long distance (<200m)
- Low reflectivity (black targets!)
- Ambient light

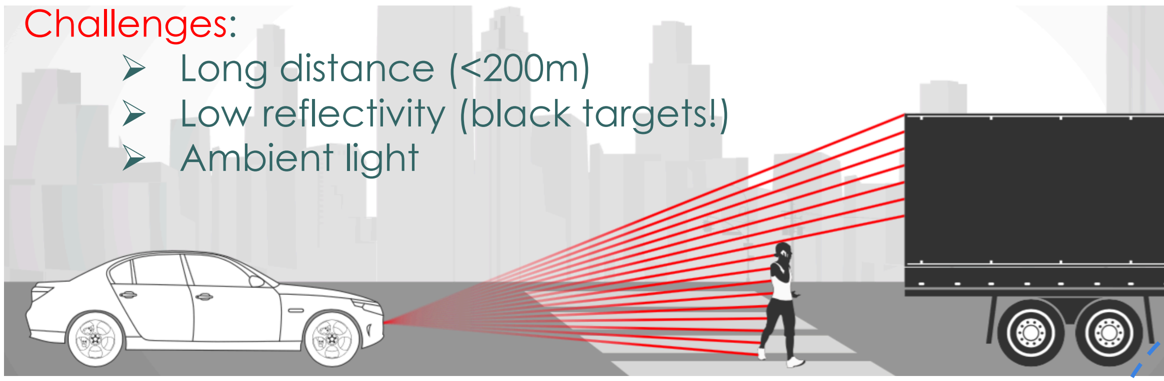

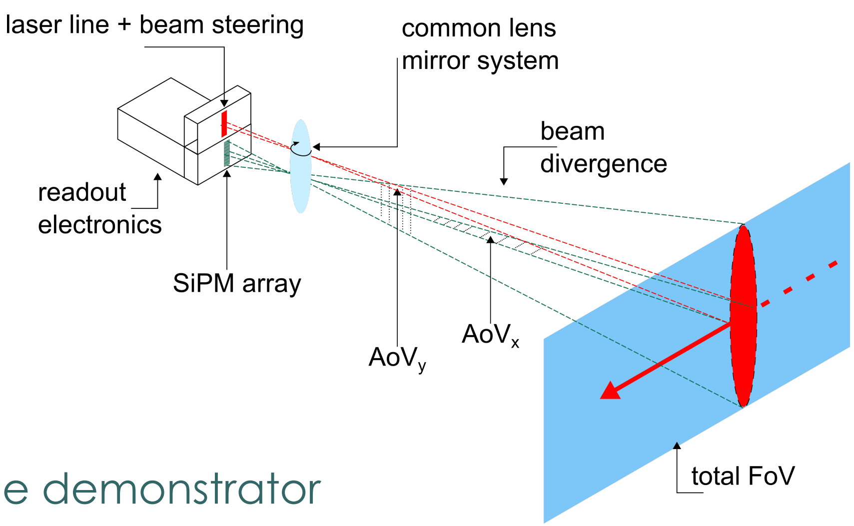

The demonstrator

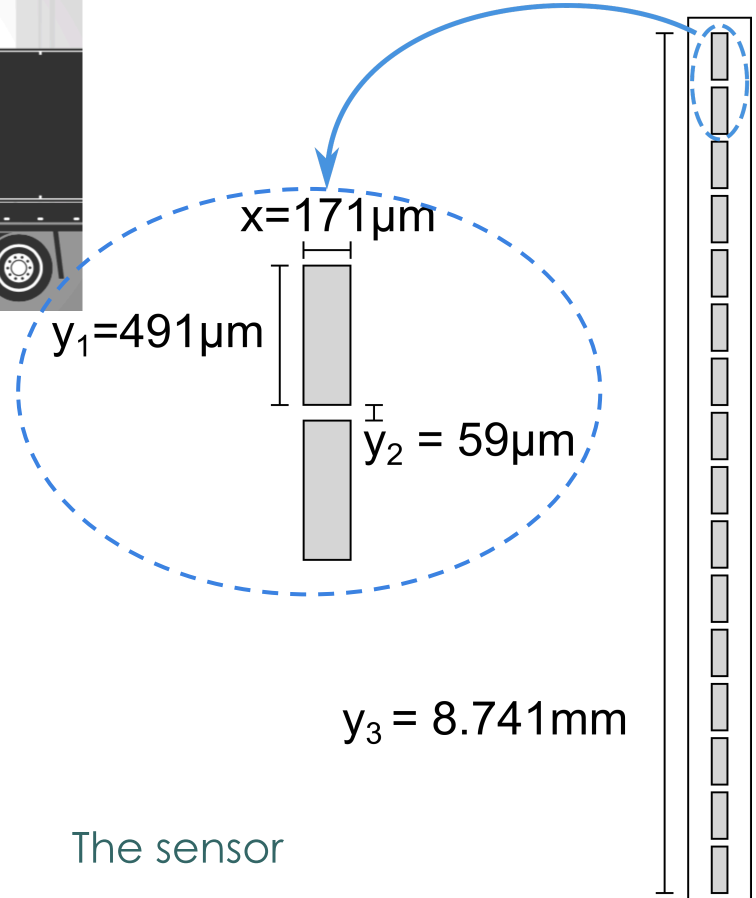

The sensor

SensL LiDAR System Parameters

Parameter	Value
Array size	1×16
SiPM pixel length x	171 µm
SiPM pixel height y_1	491 µm
Pixel spacing y_2	59 µm
Total array length y_3	8.741 mm
SPAD cells per pixel N_{cells}	133
PDE @ 905 nm	8.4 %
SPAD cell dead time τ_{dead}	23ns
SiPM pixel gain G	10^6
SiPM rise time τ_{rise}	100 ps
Laser divergence	$0.1° \times 5°$
Laser peak power P_{laser}	400 W
Laser pulse width τ_{pulse}	1 ns
Laser pulse repetition rate PRR	500 kHz
Frames per second	30 fps
Optical aperture D_{lens}	22 mm
Scanning angle of view	$80° \times 5°$
Static angle of view $AoV_x \times AoV_y$	$< 0.1° \times 5°$
Angular resolution	$0.1° \times 0.312°$
Optical bandpass $\lambda \pm \Delta\lambda$	(905 ± 25) nm

Target Detection Probability

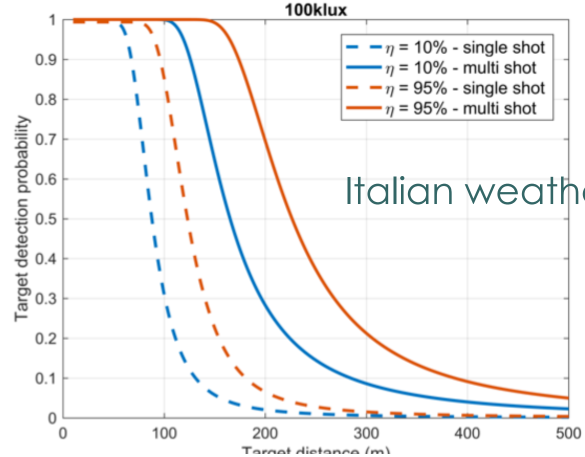

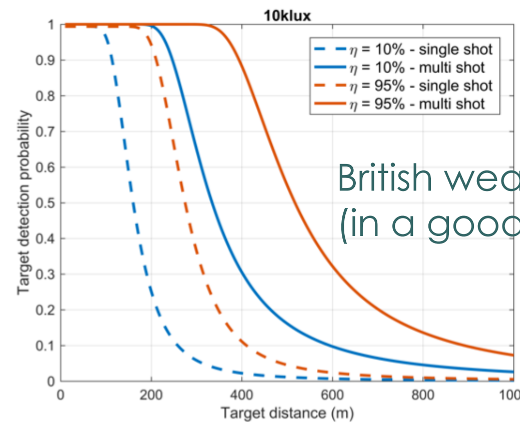

1 Lux = 1 lumen/m^2; A 25 W compact fluorescent light bulb puts out around 1700 lumen

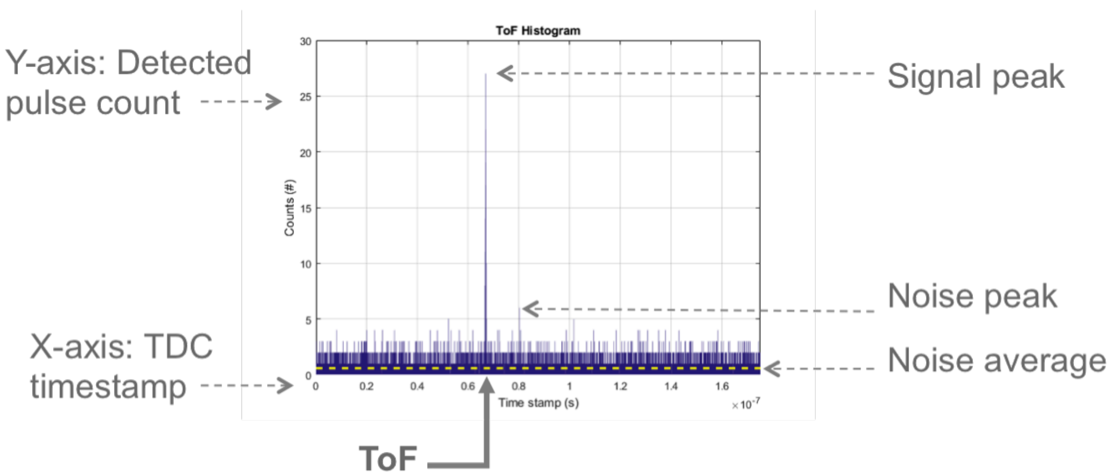

The returned signal reaches the level of the background noise, and so a multi-shot technique can be used to improve the performance and increase the probability of detection. Currently, the TOF distribution is built over 20 shots.

Philips Digital Photon Counting

http://www.digitalphotoncounting.com

- IEEE-NSS Conference record 2009 & 2010 (Thomas Frach)
- JINST 7 (2012) C01112
- D. Schaart et al., NIM A 809 (2016) 31-52

Put a bit of intelligence on board and turn the SiPM into a genuine DIGITAL device:

Active quenching, forcing the anode to the breakdown voltage

inverter, activated by the anode voltage variation, activating the the quenching mech. and identifying the cell was hit

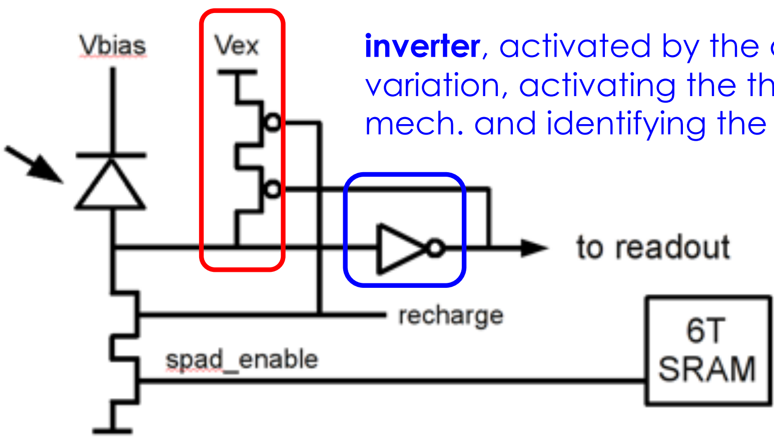

Fast recharge transistor

The 2009 chip

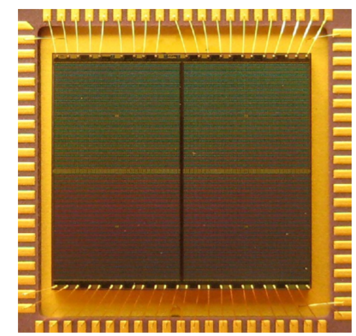

- 2 x 2 array of sensors
- 6396 cells/sensor
- 60 x 40 μm^2 cells
- chip size 7.8 x 7.2 mm^2
- peak PDE ~ 30% @430 nm
- modified 0.18 μm 5M CMOS

On ACTIVE QUENCHING, see for instance Gallivanoni et al., IEEE TRANSACTIONS ON NUCLEAR SCIENCE, VOL. 57, NO. 6, DECEMBER 2010

Exemplary illustrations of the advantages of this design:

1. Spotting hot cells and disabling their output

Since individual pixels may be enabled/disabled, the DCR of every cell can be measured, possibly identifying the HOT cells:

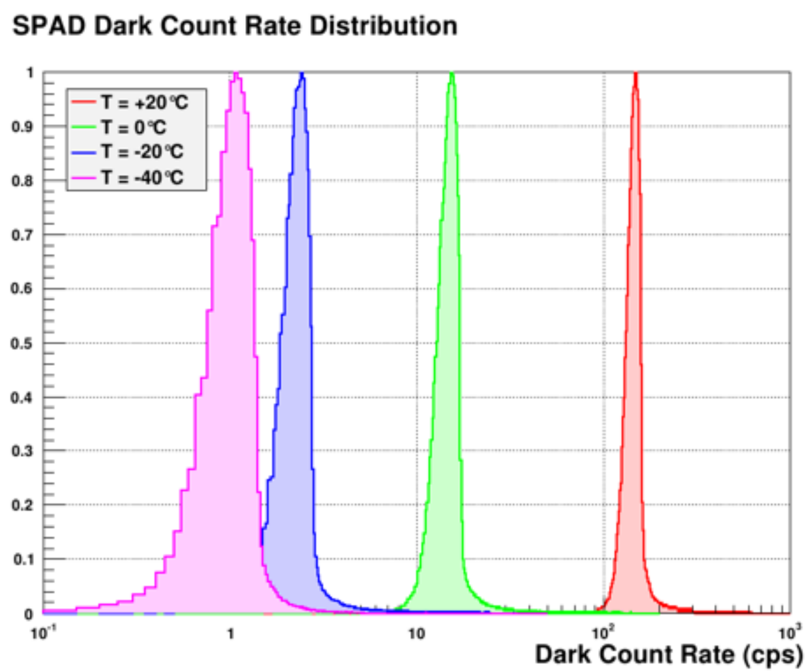

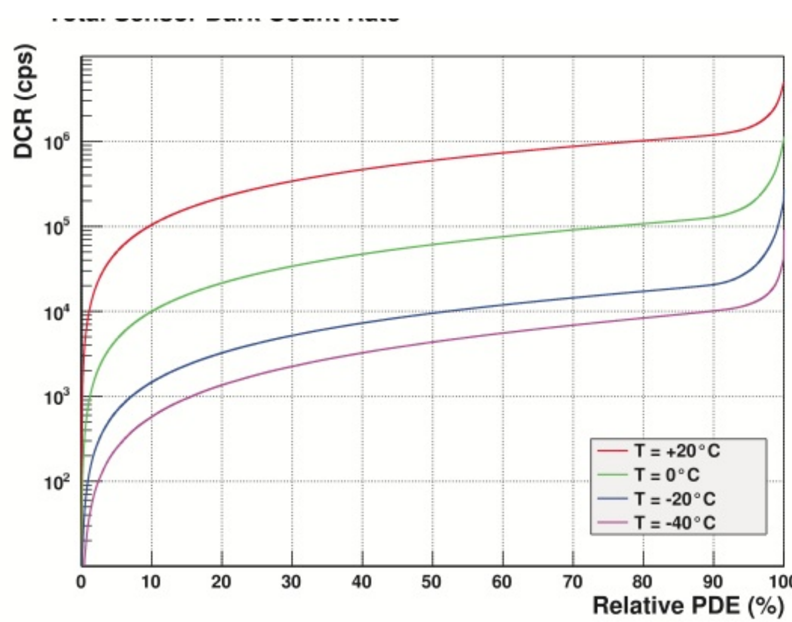

Typical dark count rate at 20°C and 3.3V excess voltage: ~150cps / diode

Exemplary illustrations of the advantages of this design:

2. Reduced temperature sensitivity

Digital SiPM are insensitive to any change in the breakdown voltage as long as the switching threshold of the gate is reached.

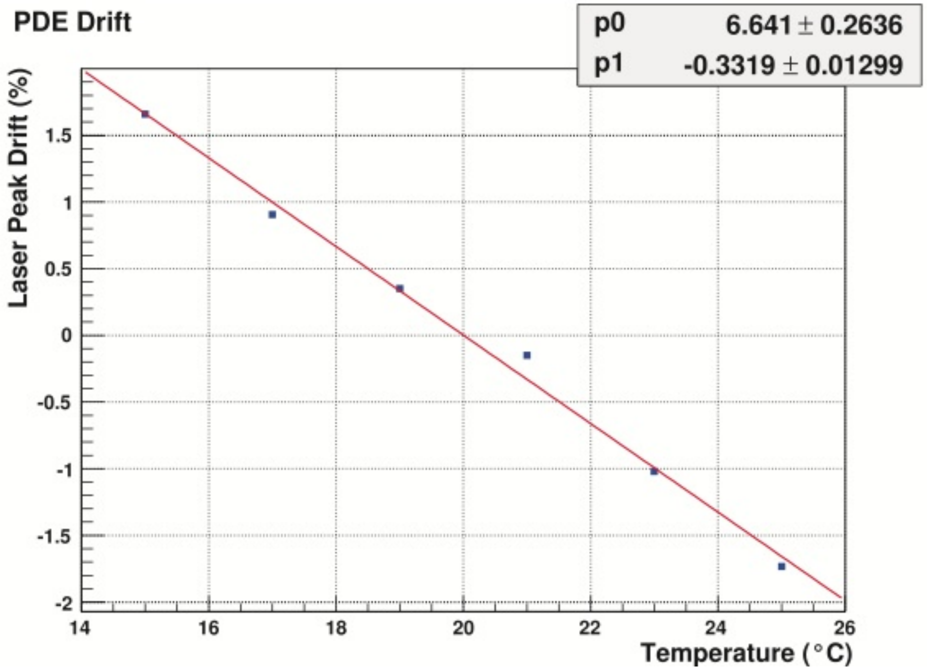

O(0.3%/C)
Vs
0.5-1%/C in standard SiPM
(operated at +5V)

The remaining drift observed in the digital SiPM is due to the change in the photon detection efficiency, caused by the temperature-dependent avalanche initiation probability.

Is it a successful device?

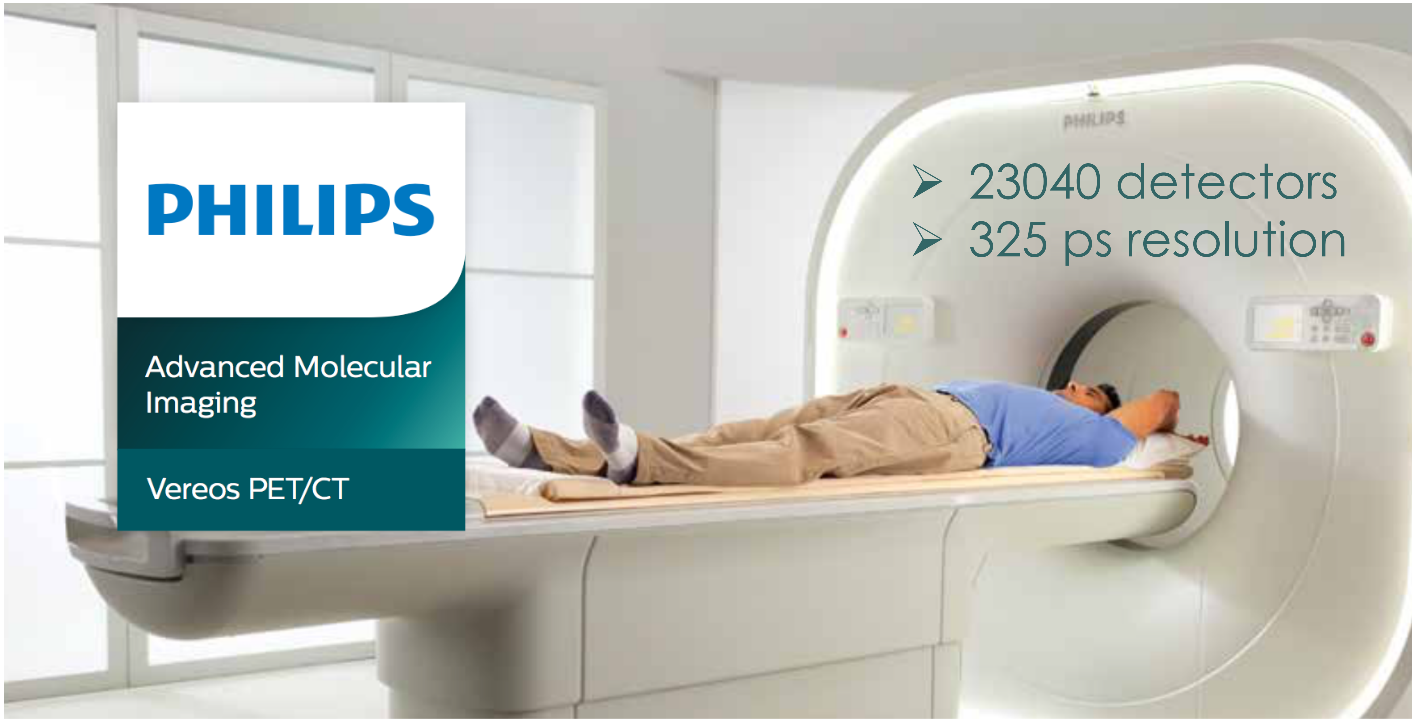

Truly **digital** PET imaging

Philips proprietary Digital Photon Counting technology

The SwissSPAD (Edoardo Charbon et al, SPAD imagers for super resolution localization microscopy enable analysis of fast fluorophore blinking, Nature Scientific RepoRts | 7:44108 | DOI: 10.1038/srep44108, 2017)

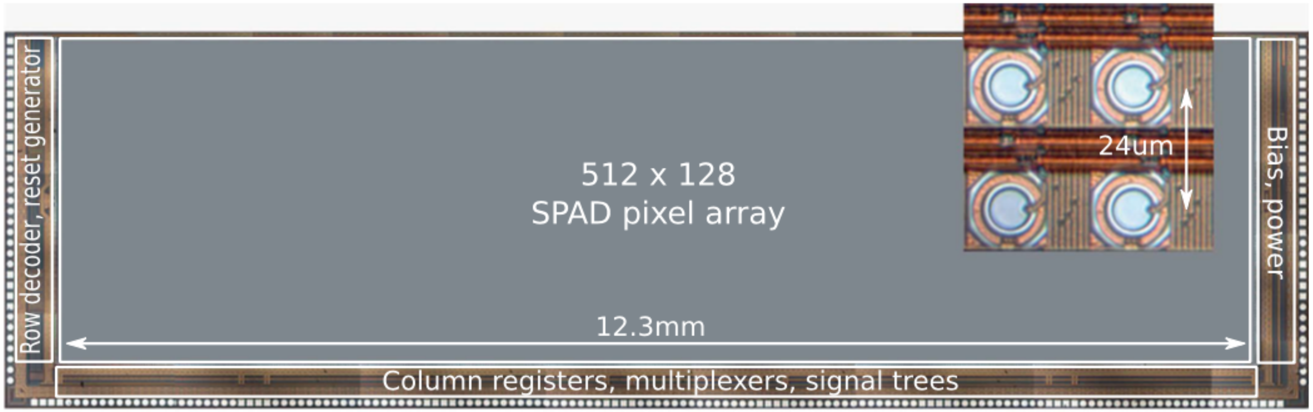

a

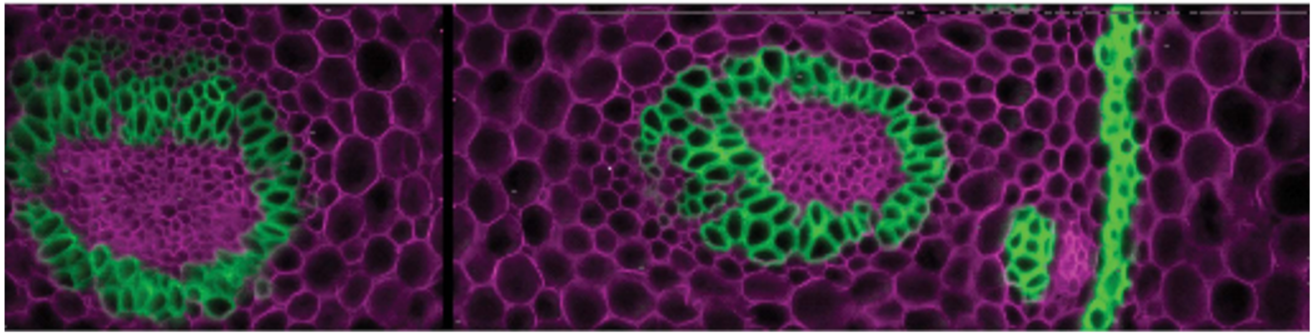

- 24 μm pixel pitch
- Rolling shutter readout (6.4 μs frame period)
- Native Fill Factor (FF) 5%
- FF enhancement by micro-lensing: 12
- Achieved super-resolution: 80 nm

The next frontier: 3D vertical integration, to turn a sensor into a SMART sensor, with intelligence on board

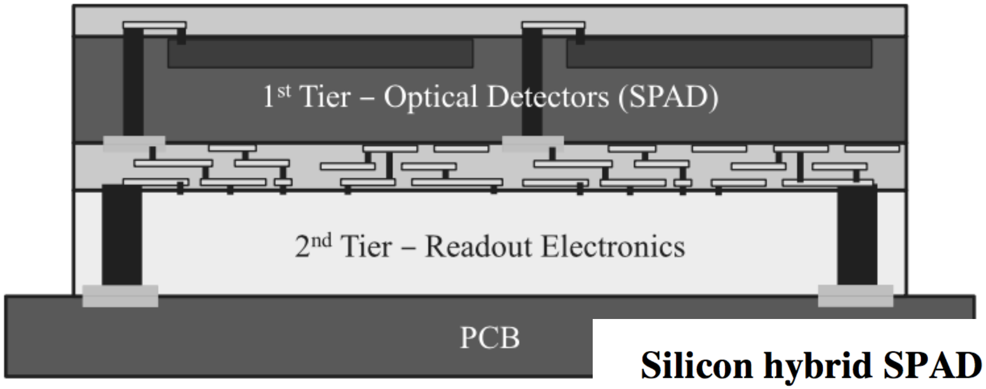

One of the latest HAMAMATSU developments

Silicon hybrid SPAD with high-NIR-sensitivity for TOF applications

Takashi Baba*[a], Terumasa Nagano[a], Atsushi Ishida[a], Shunsuke Adachi[a], Shigeyuki Nakamura[a], Koei Yamamoto[a]
[a]Hamamatsu Photonics K.K., 1126-1, Ichino-cho, Higashi-ku, Hamamatsu City, Shizuoka Pref., Japan, 433-8558

IEEE TRANSACTIONS ON NUCLEAR SCIENCE, VOL. 63, NO. 4, AUGUST 2016 2293

A 2D Proof of Principle Towards a 3D Digital SiPM in HV CMOS With Low Output Capacitance

Frédéric Nolet, Vincent-Philippe Rhéaume, Samuel Parent, Serge A. Charlebois, *Member, IEEE*, Réjean Fontaine, *Senior Member, IEEE*, and Jean-François Pratte, *Member, IEEE*

Applications (a limited number of)

❖ Pulse mode:

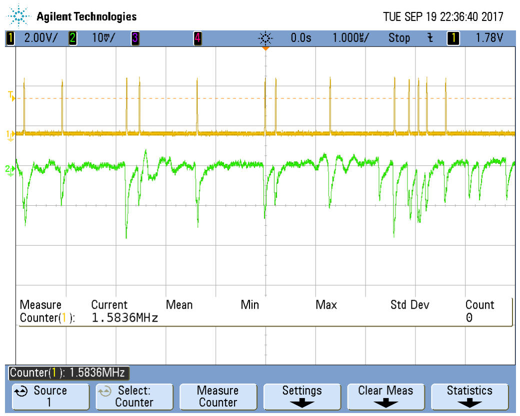

❖ Current mode:

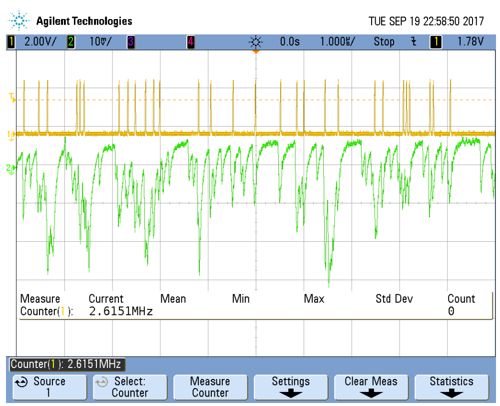

❖ Timing

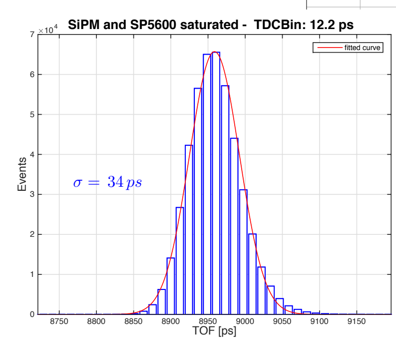

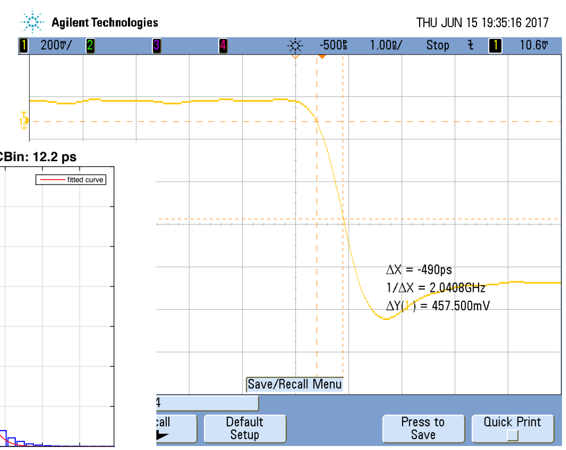

p.s. extremely biased by my activity & experience!

A Friday afternoon exercise (1/3):

Thickness measurement by β absoprtion (aka β gauging)

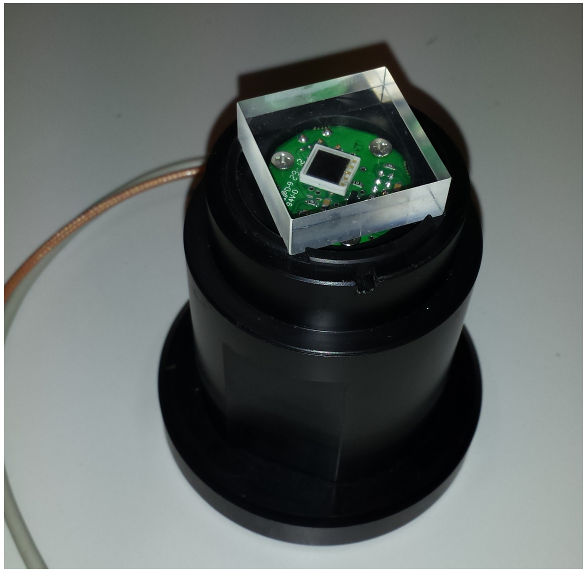

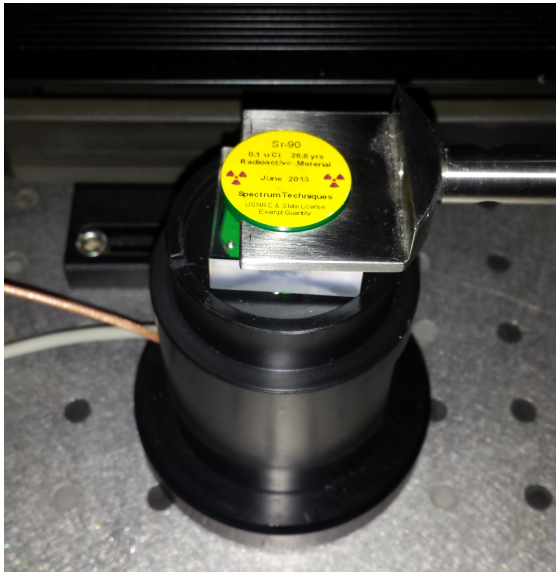

- 6x6 mm^2 SiPM
- 1 cm thick plastic scintillator

- 37 kBq ^{90}Sr source

- post-it sheets
  interleaved between the source and the scintillator

Can I count the number of sheets by the counting rate?

A Friday afternoon exercise (2/3):
Thickness measurement by β absoprtion (aka β gauging)

Counting frequency

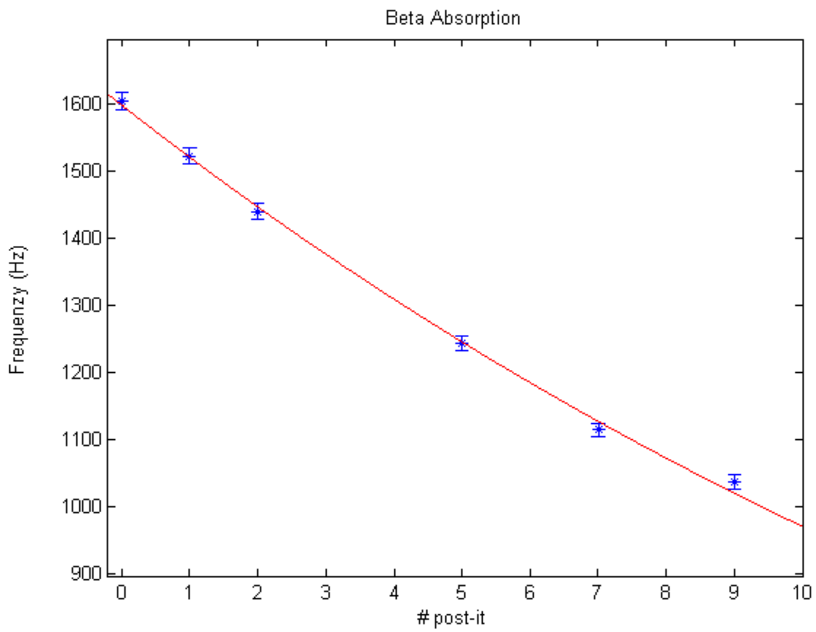

No. post-it sheets

$$\nu = ae^{-bn}$$

a = 1600 Hz
b = 0.05
n = number of post-it sheets

→ in 250 ms I can tell you at 3σ level if I have 1 or 2 post-it
→ In 25'' I can detect a thickness variation at the 10% level

Is it serious?

A Friday afternoon exercise (2/3):

Thickness measurement by β absoprtion (aka β gauging)

Radioisotope sensor for measuring the density of paper and cardboard web based on the isotope Kr 85 A361 CAN LEB1

Brief description

Radioisotopic density sensor of sheet materials A361 CAN (LEB-1) is designed for use in automated quality control system "A-3000" for the continuous and non-contact technological control paper web density or other sheet materials.

Application range — paper web density continuous monitoring for the papermaking and other sheet materials process control.

5014i Beta Continuous Ambient Particulate Monitor

Measure PM-10, PM-2.5 or PM-1 mass concentrations with the Thermo Scientific™ 5014i Beta Continuous Ambient Particulate Monitor. The 5014i distinguishes itself from other beta measurement methods by utilizing a continuous (non-step wise) mass measurement with a proven industry standard which provides for long-term unattended operation. To accurately address potential water bias and volatile loss, the Dynamic Heating System allows the user to hold the sample temperature at a fixed value or below a relative humidity threshold.

Radiation Protection – an exemplary illustration for the UK

The TN15™ high sensitivity thermal neutron detector utilizes a state-of-the-art Silicon photomultiplier (SiPM) and offers world-leading specification in a compact form. The TN15™ surpasses the performance of a 100mm long 13mm ^3He tube at 4 atmospheres.

Specifications:	
Equivalent to 100mm x 13mm Ø ^3He at 4 atmospheres	
Photo-sensor	SiPM array
Thermal Neutron Sensitivity	>50%
Maximum throughput	10,000 cps
Power consumption	250 mW
Dimensions	131mm x 33mm x 24mm
Weight	110 gram
Temperature range	-10 to 40°C

TN15 ™ by KROMEK, Sedgefield
County Durham, UK
www.kromek.com

The 2015 blockbuster

D3S

- Compact Bluetooth gamma neutron detector for $400
- All technology available at OEM level
  - Gamma module
  - Neutron module
  - Bluetooth MCA
    - All designed for ultra low power
- All software can be supplied badged or further developed as required
  - Android application
  - Fully secure web application including GPS

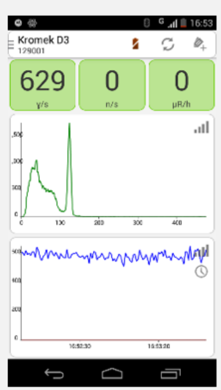

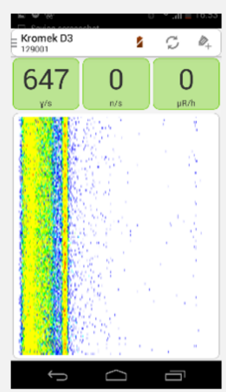

RadioGuided Surgery (RGS)

1. F Bogalhas et al., Phys. Med. Biol. 54 (2009) 4439–4453
2. Solfaroli Camillocci et al., NATURE SCIENTIFIC REPORTS | 4 : 4401 | DOI: 10.1038/srep04401 (2014)
3. H. Sabet et al., IEEE TRANSACTIONS ON NUCLEAR SCIENCE, VOL. 62, NO. 5, OCTOBER 2015

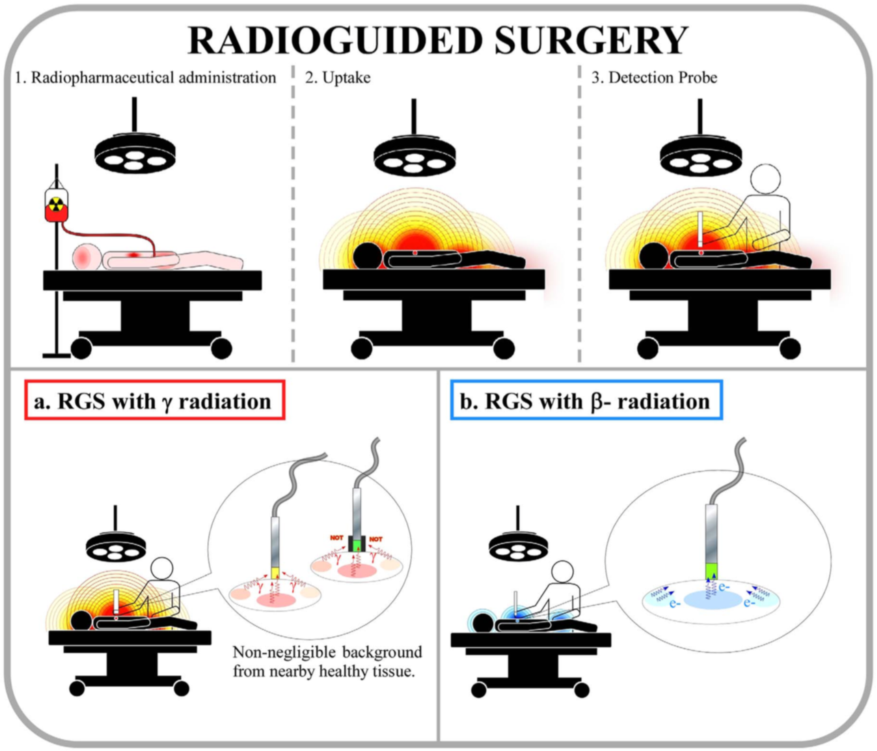

The precise localization and complete surgical excision of tumors are one of the most important procedures in the treatment of cancer. In that context, the goal is to develop new intra-operative probes to help surgeons to detect malignant tissues previously labeled with β or γ radiotracers.

RGS with β^- (ref.2)

Focused on brain tumor (meningioma) for two reasons:

- It is particularly receptive to synthetic somatostatin analogues, such as DOTATOC, that can be labelled with the β^- emitting ^{90}Y
- The concentration of "standard" β^+ emitting isotopes (e.g. 18F-FDG used for PET) is quite high in the brain, inducing a significant background

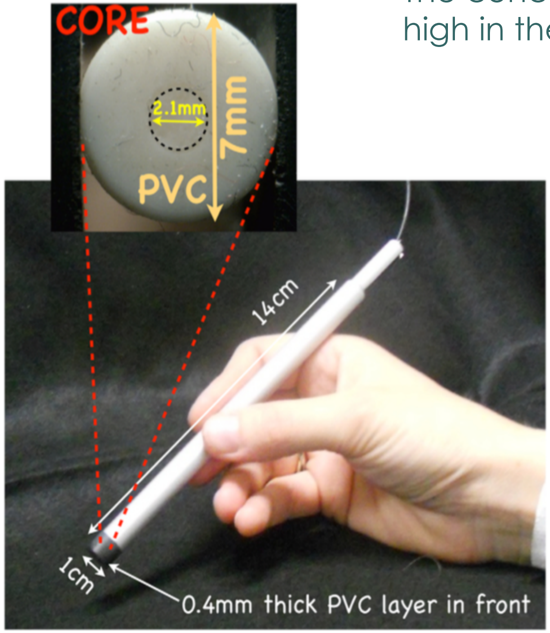

Figure 2 | First prototype of the intraoperative β^- probe. The core is a cylindrical scintillator (diameter 2.1 mm, height 1.7 mm) of poli-crystalline p-terphenyl. A ring of PVC wraps the scintillator and shields it against radiation coming from the sides. The device is encapsulated inside an easy-to-handle aluminum body as protection against mechanical stress and it is protected against light by a thin PVC layer.

Results from phantoms with a specific activity corresponding to what can be expected in clinical applications

Phantom	Diameter (mm)	Height (mm)	Volume (ml)	Rate (cps) 22 kBq/ml	T (s) 22 kBq/ml	Rate (cps) 5 kBq/ml	T (s) 5 kBq/ml
Residual	6	3.5	0.10	31.6	1	6.6	2
H1	4	1	0.01	12.4	2	2.6	>10
H2	4	2	0.02	17.7	1	3.7	4
H3	4	3	0.04	20.1	1	4.2	4

Time required to get False Negative < 5% and False Negative ≈ 1%

RGS with β^+ (ref.3) (1/2)

An IMAGING DEVICE engineered to detect β^+ emitting isotopes irrespective from the γ background

❖ Conceptual design & prototype of the probe

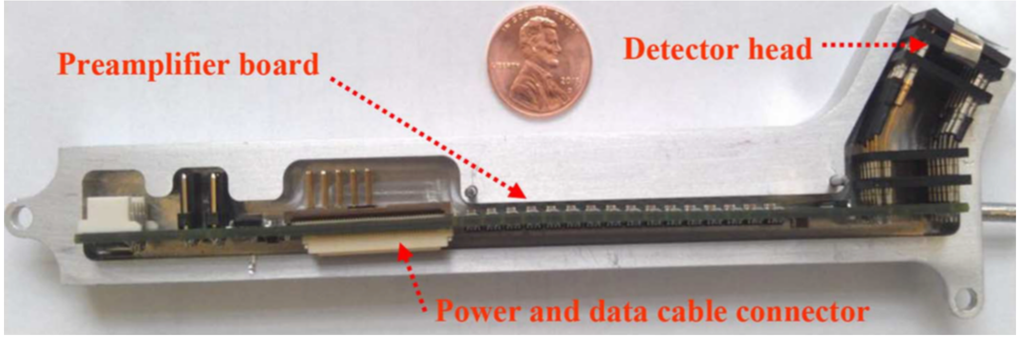

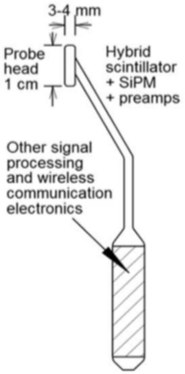

❖ A head designed to identify and discriminate β^+ from γ

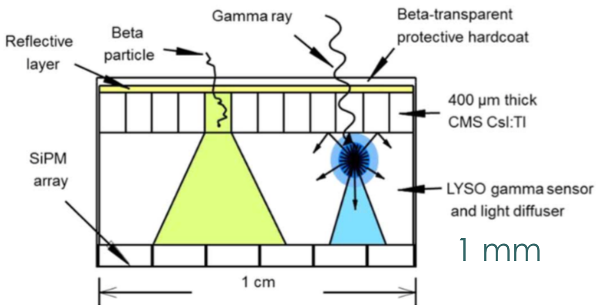

- CsI to detect β^+ rather than plastic scintillator for the light yield (53 photons/keV vs 10 photons/keV); $\bar{E}_{\beta^+}$= 250 keV, E_{max}= 635 keV
- β^+ vs γ discrimination profiting from the difference in the time constant of the CsI (800 ns) vs LYSO (40 ns)

RGS with β^+ (ref.3) (2/2)

Images of a ^{18}F droplet ($\approx 1mm\ diameter$) @different background levels

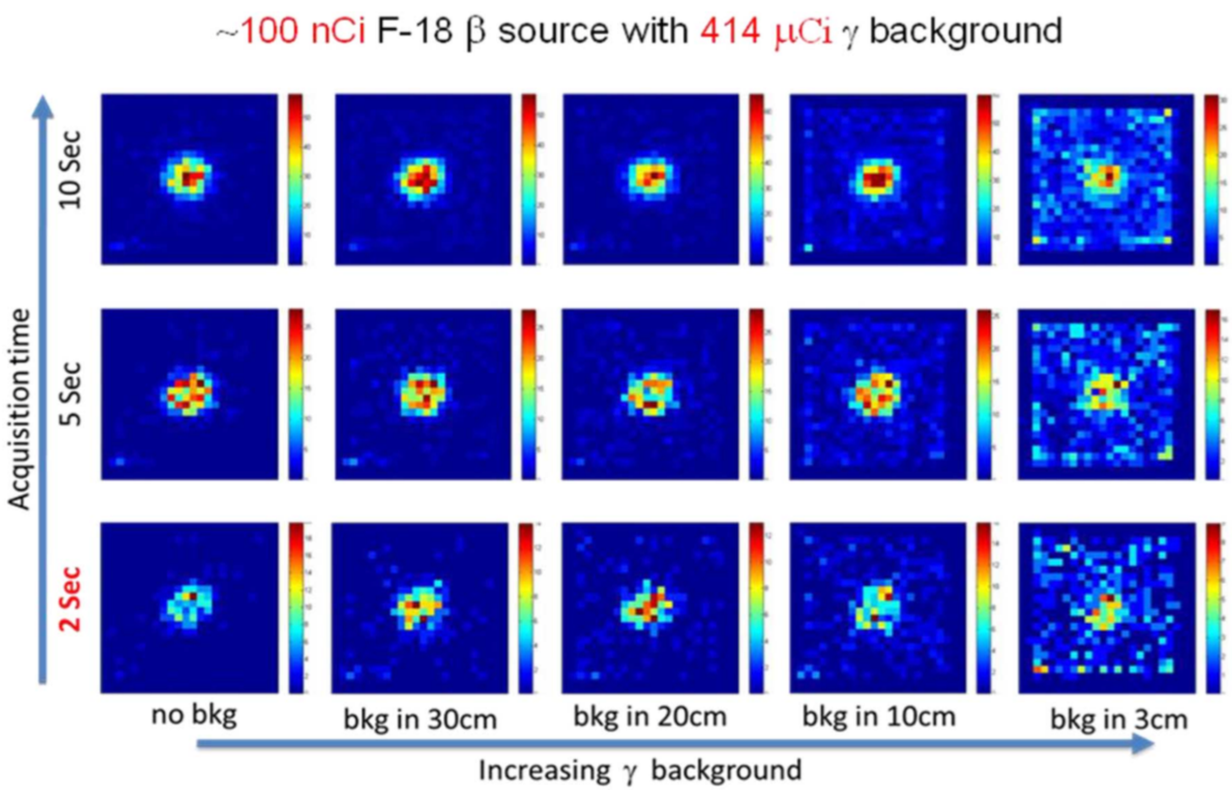

Still a bit qualitative (on spatial resolution and sensitivity) but definitely intriguing

Response to a constant flux: Dosimetry in mammography

C. Cappellini et al., 2008 IEEE Nuclear Science Symposium Conference Record & NIM 607 (2009), 75–77

Dosimetry in mammography is utmost important and this is somehow proven by the ongoing debate on the relevance of mammography screening

…but currently existing instruments are limited:

- Standard Termo-Luminescent Detectors require to be analyzed after examination, degrade with time
- MOSFET detectors suffer from low stability and degrade with each irradiation
- Ionization chamber devices need relatively high voltage (cannot be used in contact with the patient), not tissue equivalent

precise measurements of the actual dose being received by a patient without distorting the X-ray beam and introducing any artefacts in the image

Some functional requirements:

- dose rate range (2 ÷ 150 mGy/s)
- dose range (0.5 mGy - 180 mGy)
- sensitivity (5%)
- overall accuracy (±10%)
- tolerance to environmental variation & stability

Prototype qualification

Conceptual design of the prototype tested @ PTW – secondary standard lab for dosimetry:

Scintillator

(tile or fiber)

Ligth guide
Ø 1 mm
clear fiber

FC connector &
SiPM

Electronics

PHISYCAL OBSERVABLE:
"buffered" signal sum

Sum of samples signals selected by an edge detector algorithm + left & right buffer

⇒ proportional to the DOSE

Trace plot: typical mammo SiPM output
(continuous photons flux – pulse duration of each sample100 ms)

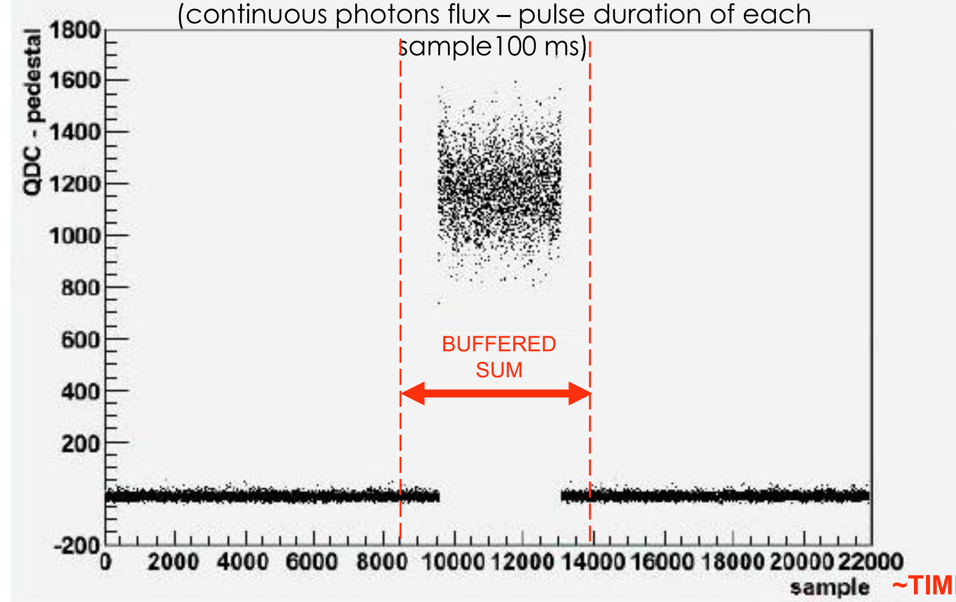

summary of the results

Two different set-up (optimized for dynamic range & λ):

- 1mm scintillator tile
- Blue scintillator fiber

coupled with MPPC (400 cells, 1x1 mm^2)

Irradiation: 0,22 ÷ 217 mGy/s

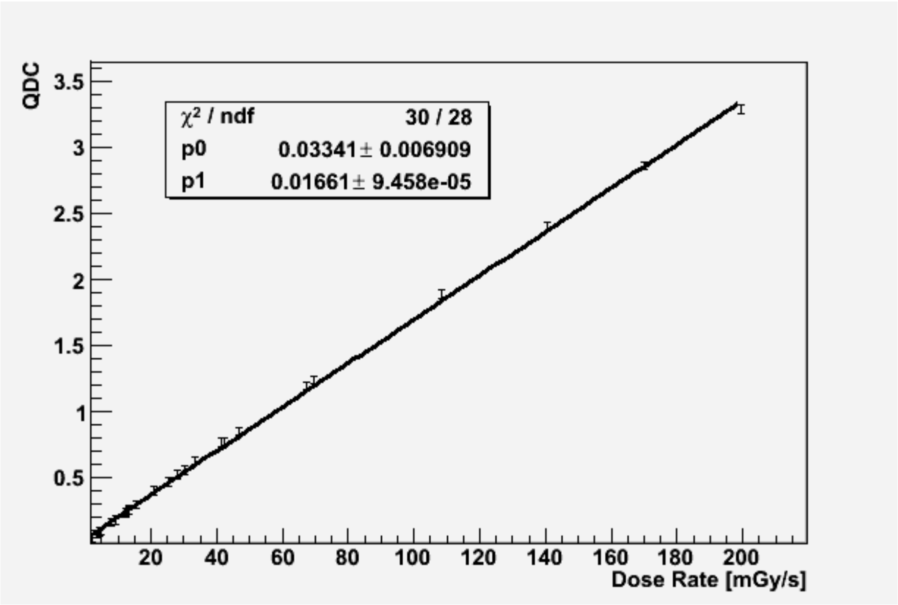

	Fiber + Hamamatsu MPPC
Precision(%)	2.31 ± 0.03
Sensitivity^A (mGy/s)	2.05 ± 0.03
MDS^B (mGy/s)	0.458 ± 0.007
Linear Dinamic range (mGy/s)	> 200

^{A}Sensitivity: Precision / system gain

^{B}MDS: minimum signal distinguishable from the noise

Time-of-flight Positron Emission Tomography (TOF-PET) & LIDAR

M. Conti, Physica Medica (2009) 25, 1-11

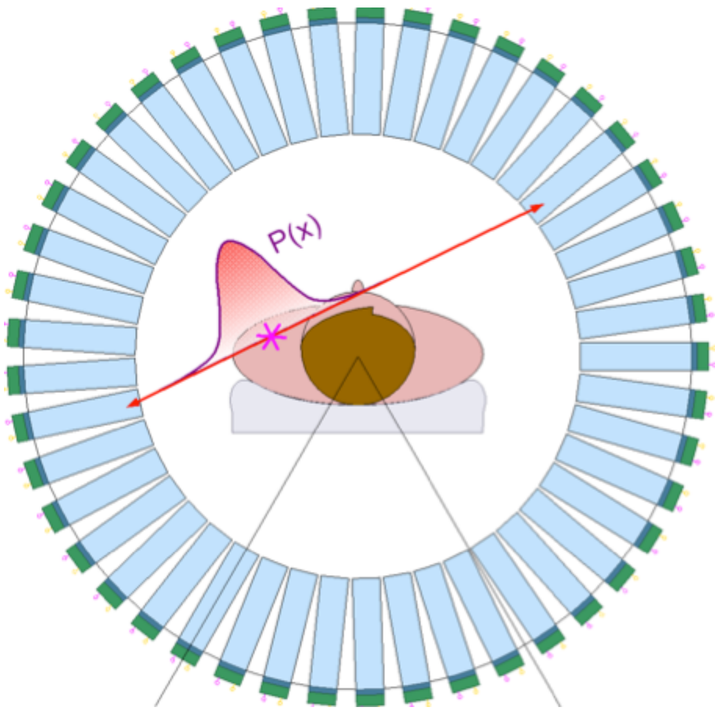

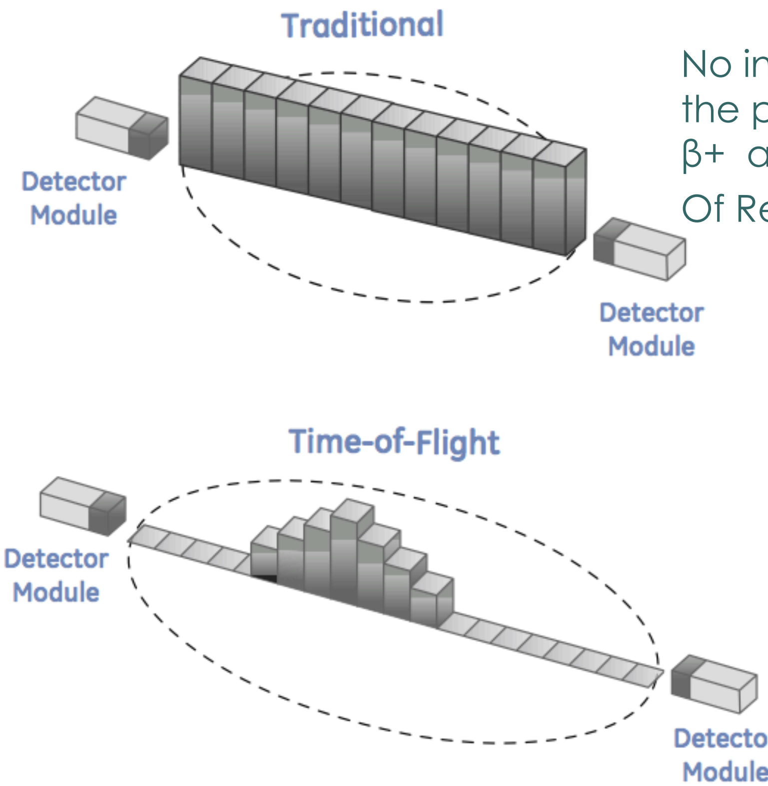

No indication about the position of the β+ along the Line Of Response (LOR)

The functional imaging tool, based on the detection of pair of γ rays emitted back-to-back by the annihilation of the β+ emitted by the ^{18}F, chemically bound to FDG

Identify the position of the β+ along LOR by the differenc ein the time of arrival of the photons

TOF-PET is a HOT topic: 1510 papers in 2008-2013 (Google Scholar) + significant investments by funding agencies & companies

The gain in the image quality between a conventional and a TOF-PET system may be quantified as [Conti]:

$$G = \frac{SNR_{TOF}}{SNR_{non-TOF}} = \sqrt{\frac{D}{c*CTR}}$$

- D = volume being inspected
- c = speed of light
- CTR – Coinicidence Time resolution

CTR	G	
1 ns	1.6	
500 ps	2.3	← Current machines
100 ps	5.2	← TARGET

[S. Gundacker et al., NIM A 737 (2014) 92–100]

SiPM do play a role, since the timing resolution of a sensor my roughly be written as:

$$\sigma_t = (output\ signal\ fluctuations)/(signal\ slope)_{trigger}$$

Exemplary illustration of results obtained with the HAMAMATSU SiPM [R. Vinke et al. NIM A 610 (2009) 188–191]:

Time resolution wrt a laser shot (worth thinking of it for ranging & LIDAR)

[1x1 mm^2, 50 micron cell pitch]

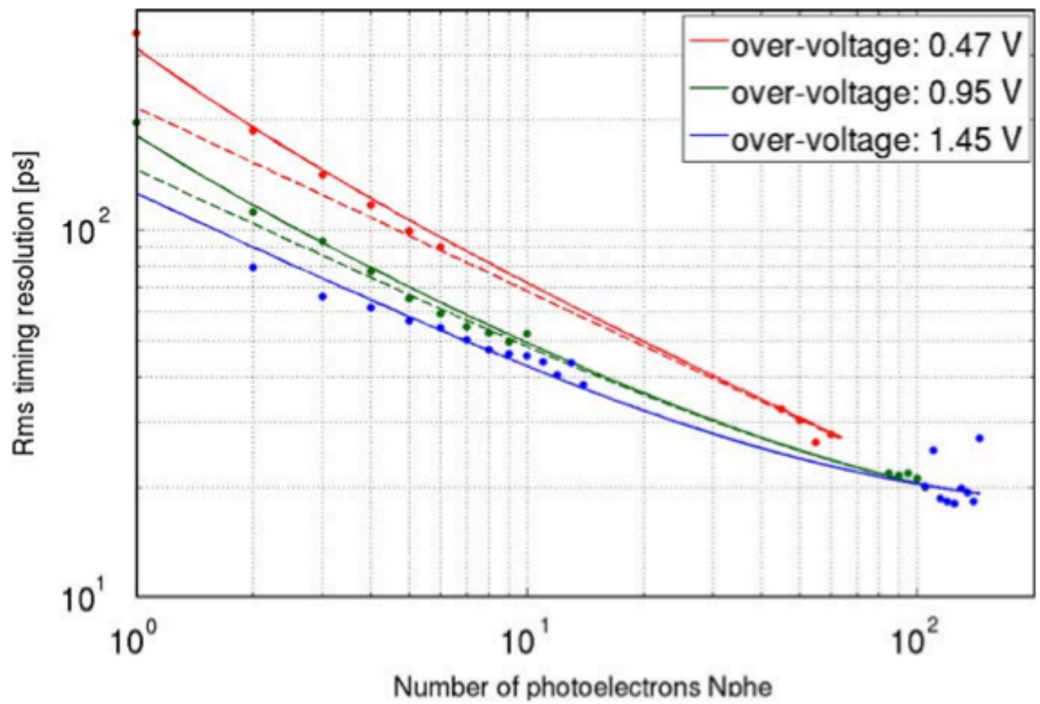

Currently, a SInglePhotonTimingResolution ≈ 35 ps has been reported (Acerbi et al., IEEE Transaction in Nuclear Science, 10.1109/TNS.2014.2347131

Timing properties of the sensor are not the full story and the scintillator does play a role [S. Gundacker et al., NIM A 737 (2014) 92–100]:

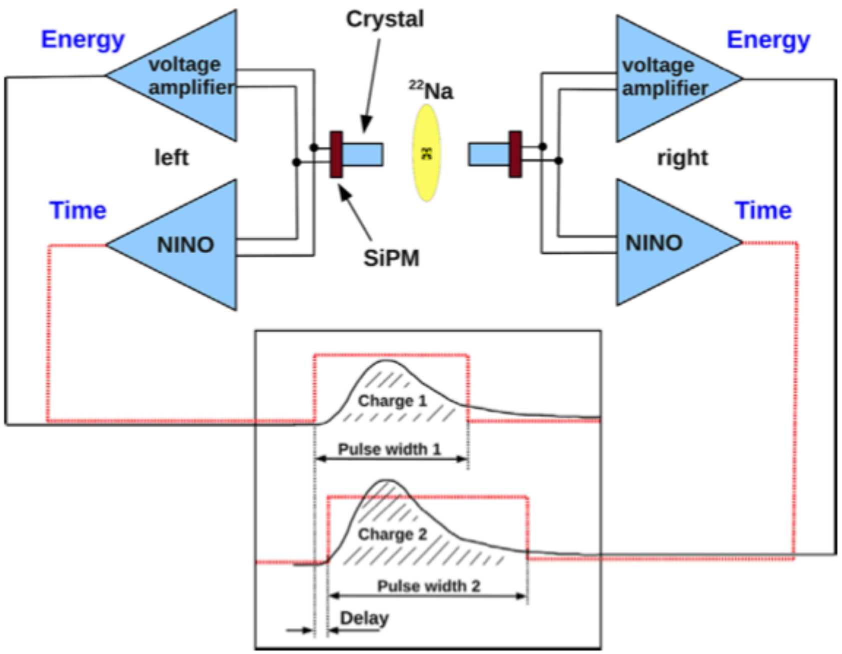

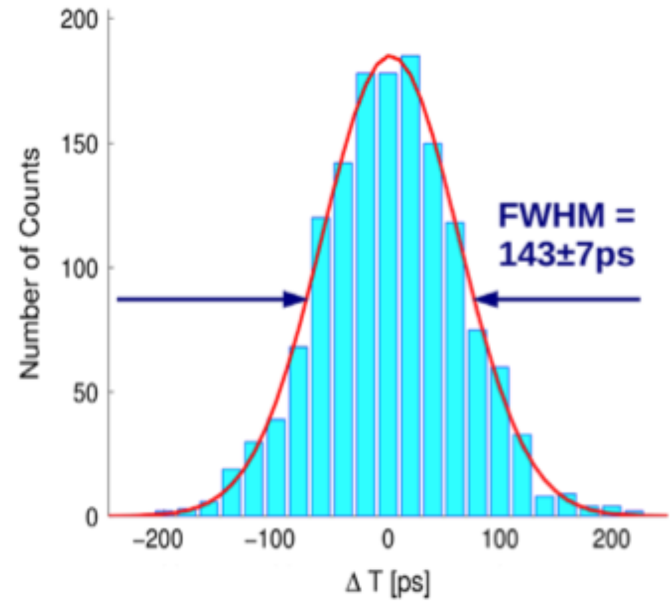

•[3x3 mm^2, 50 micron cell pitch]
• 2x2x10 mm^3 LSO crystal

Actual resolution, accounting as well for the Photon Travel Spread (PTS) resulting by the point-of-interaction and scintillation light time spread

Small animal PET/CT scanning is also a significant market

(valued $790 million in 2012, and estimated to grow at an annual growth rate of 14.5% over the next five years)

- The price for different small-animal PET systems ranges between $400,000 and $1,200,000, depending on the PET system configuration

- No. of crystals/scanner:~ 30000

medicalphysicsweb

RESEARCH • TECHNOLOGY • CLINICAL APPLICATIONS

Home | Opinion | Newsfeed | Research | Journals | Multimedia | Jobs | Buyer's guide | Events | Contact

LATEST NEWSFEED ARTICLES

- Elekta CE Marks Leksell Gamma Knife Icon
- Oncology professionals discuss

NEWSFEED

Mar 3, 2015

University of Tübingen, Mediso to develop preclinical PET insert for simultaneous PET/MRI

JOURNAL OF NUCLEAR MEDICINE TECHNOLOGY • Vol. 40 • No. 3 • September 2012

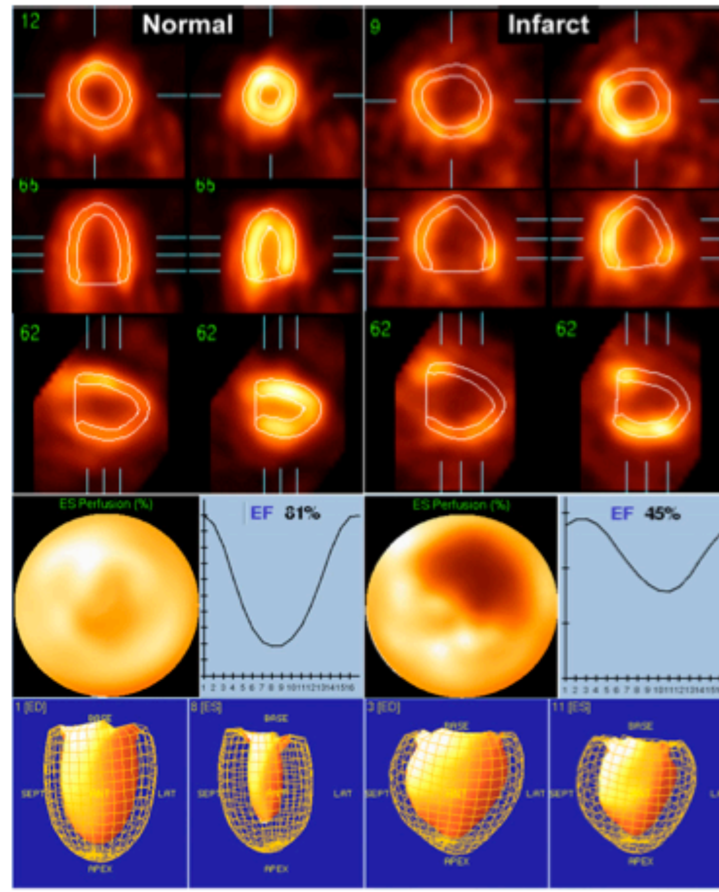

FIGURE 5. Electrocardiogram-gated ^{18}F-FDG studies in normal and infarcted rats obtained using clinical cardiac analysis software QGS (56). Polar maps display end-systolic ^{18}F-FDG uptake. Ejection fractions for normal and infarcted rats are 81% and 45%, respectively. ED = end-diastolic; EF = ejection fraction; ES = end-systolic. (Adapted with permission of (55).)

the easyPET concept *

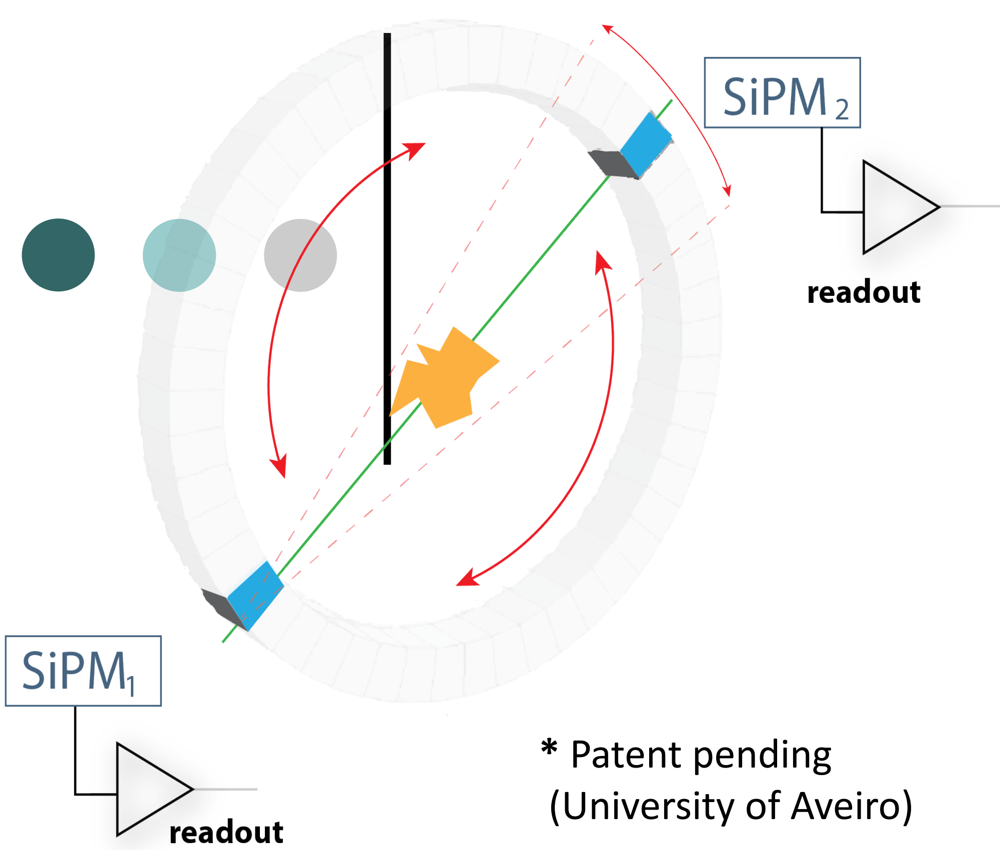

* Patent pending
(University of Aveiro)

- based on a single pair of detectors (LYSO + SiPM)
- detectors mounted on rotating structure with 2 degrees of freedom, allowing reconstruction of source position
- axial FOV: small animals (mice/rats)
- system geometry removes parallax errors, eliminating the need of DOI measurement
- allows highly granular detector assemblies for enhanced performance

easyPET provides a very cost-effective solution for entry level systems, due to the extreme reduction in the nr. of detectors and complexity of the overall apparatus

current status:

fully functional
educational system developed *

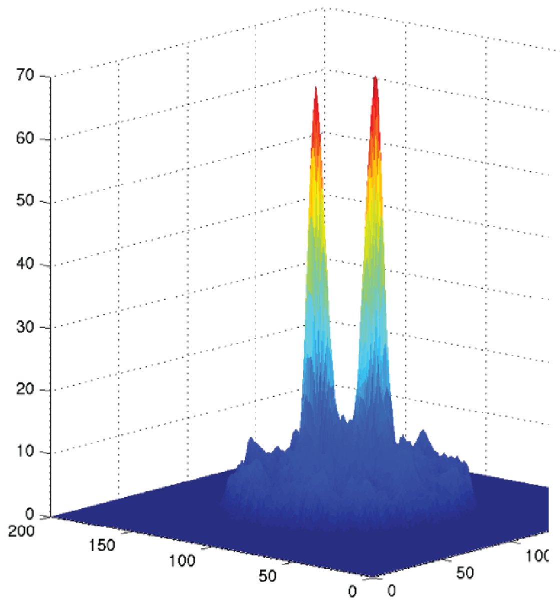

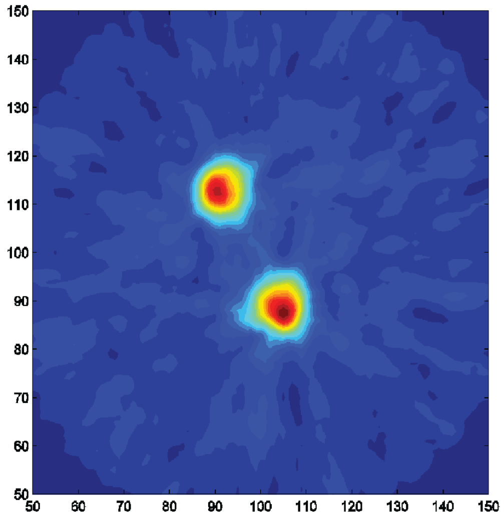

- 2D prototype designed, engineered and commissioned
- Arduino UNO microcontroller
- MATLAB interface: control and online imaging
- Two ^{22}Na sources, 5 µCi
- 2.7 mm Ø, 9 mm apart
- forward projection (no filtered reconstruction)
- position resolution < 1.5 mm FWHM, uniform over the whole FOV

* Licensing under way for didactic/educational purposes

universidade de aveiro

partners:

UNIVERSITAS STUDIORUM INSUBRIAE

CAEN Tools for Discovery

Last but not least: High Granularity Calorimetry for High Energy Physics [the domain of CALICE, even if we also entered the game]

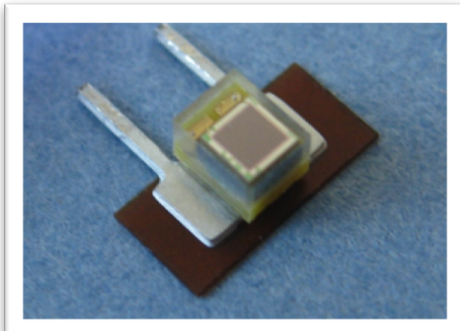

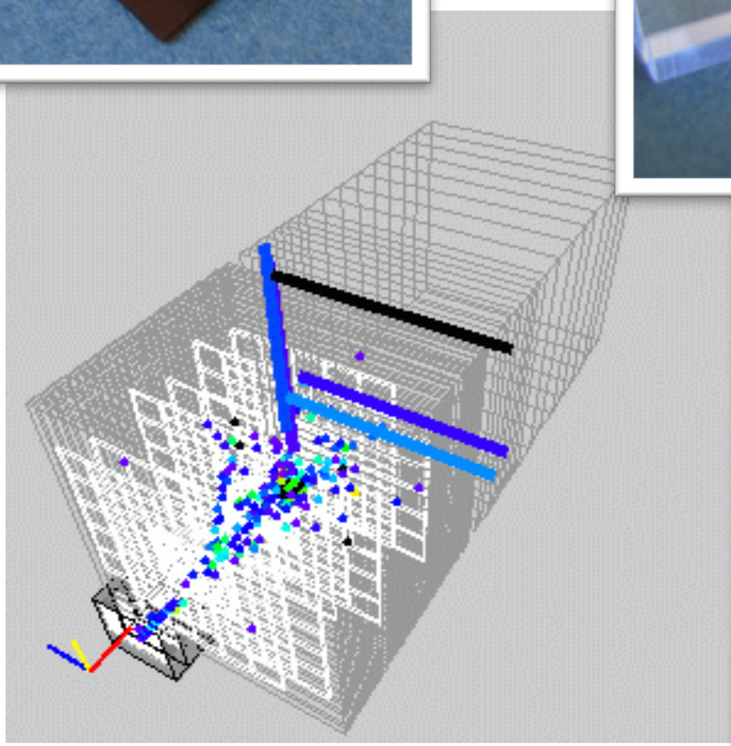

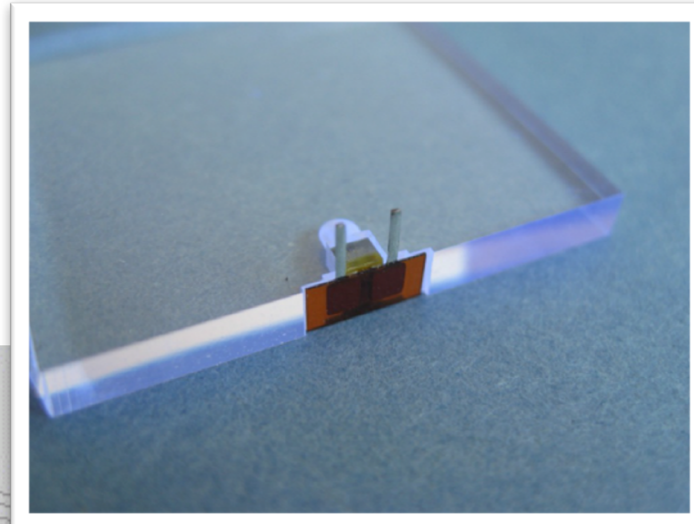

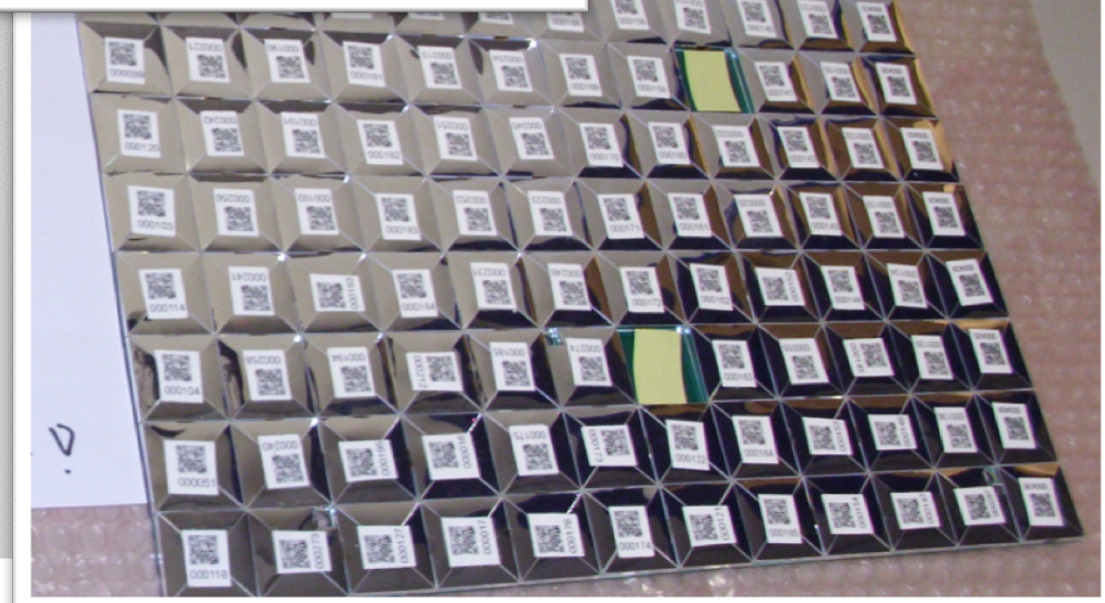

A SiPM based Dual Readout Calorimeter module (DREAM)
(http://highenergy.phys.ttu.edu/dream/)

A small DREAM by now…

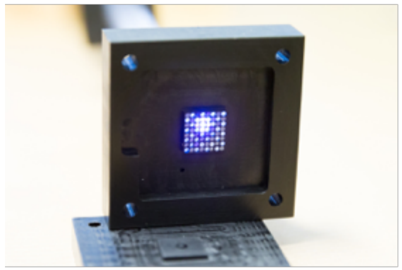
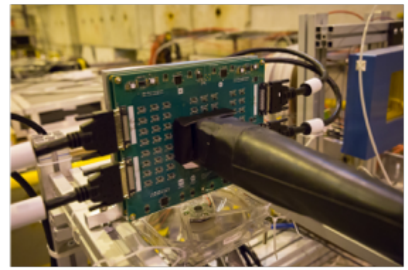
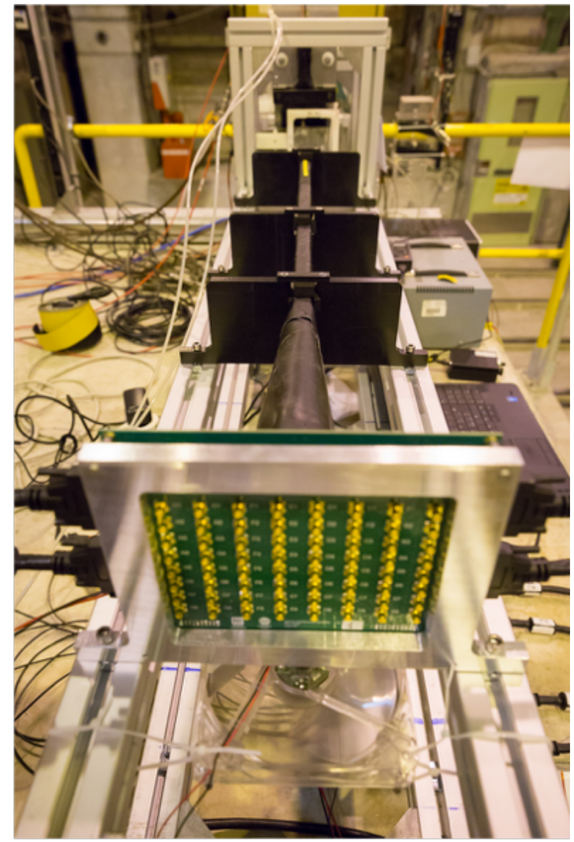
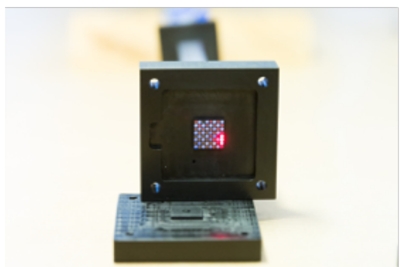
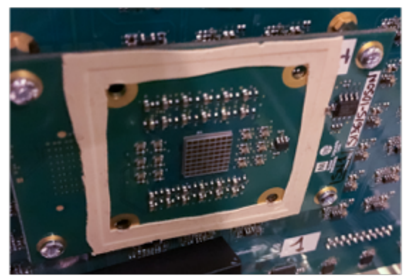
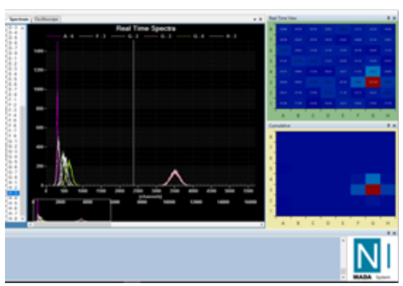
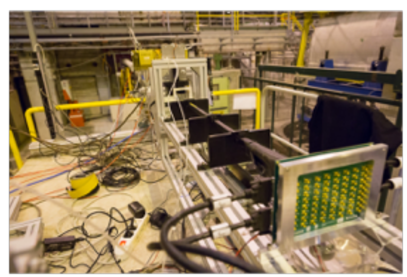

on beam at CERN in October 2016 & July 2017

And we made it (and the best is yet to come)!

Centered

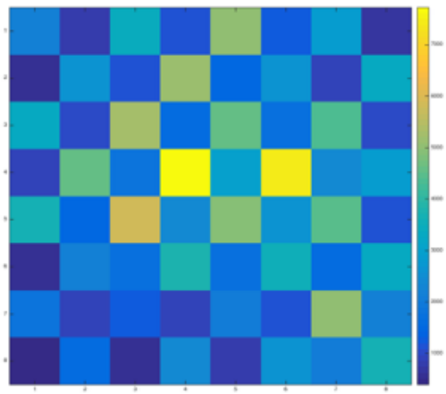

Off-centered

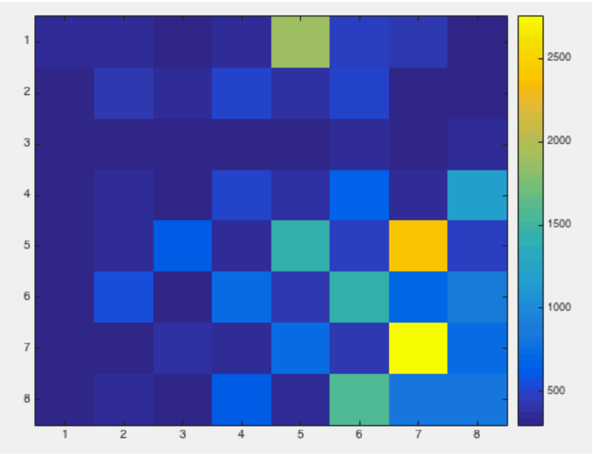

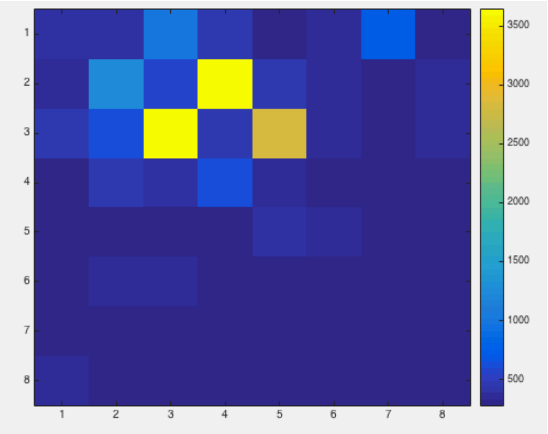

40 GeV electrons

A muon

What did we do since we got started with SiPM, in 2006?

- RAPSODI, a Framework Program 6 EC project:
  - Real-time dosimetry in mammography (with PTW-Freiburg)
  - Indoor radon concentration (with JP-SMM, Cz)
  - Gamma detection for security (with FORIMTECH-CH)

- Partnership with CAEN.s.p.a. for the development of a SiPM kit for Science & Education (http://www.caentechnologies.com/jsp/Template2/CaenProd.jsp?parent=61&idmod=1023)

- MODES-SNM, a Framework program 7 EC project on Homeland Security (ARKTIS detectors & CAEN)

- Two Homeland security projects [KROMEK, AWE (UK Atomic Weapons establishment)]

- Dual Readout Calorimetry (Texas Tech, Iowa State Uni., INFN, Nuclear Instruments)

- Radio-guided surgery (Light Point Medical, UK, completed)

- EasyPET 2D with CAEN and University of Aveiro (3D on the way)

- Dual Energy Bone densitometry (partnership with an Italian Company)

- Industrial Automation (Partnership with a Swiss company)
- Chemiluminescence (in partnership with 2 research institutions from Italy)
- Dosimetry and QC of radiotherapy machines with scintillating fibers (Ireland)
- “friendly” relationship with HAMAMATSU Europe & the other producers

Take Home Message: when you see a wave…

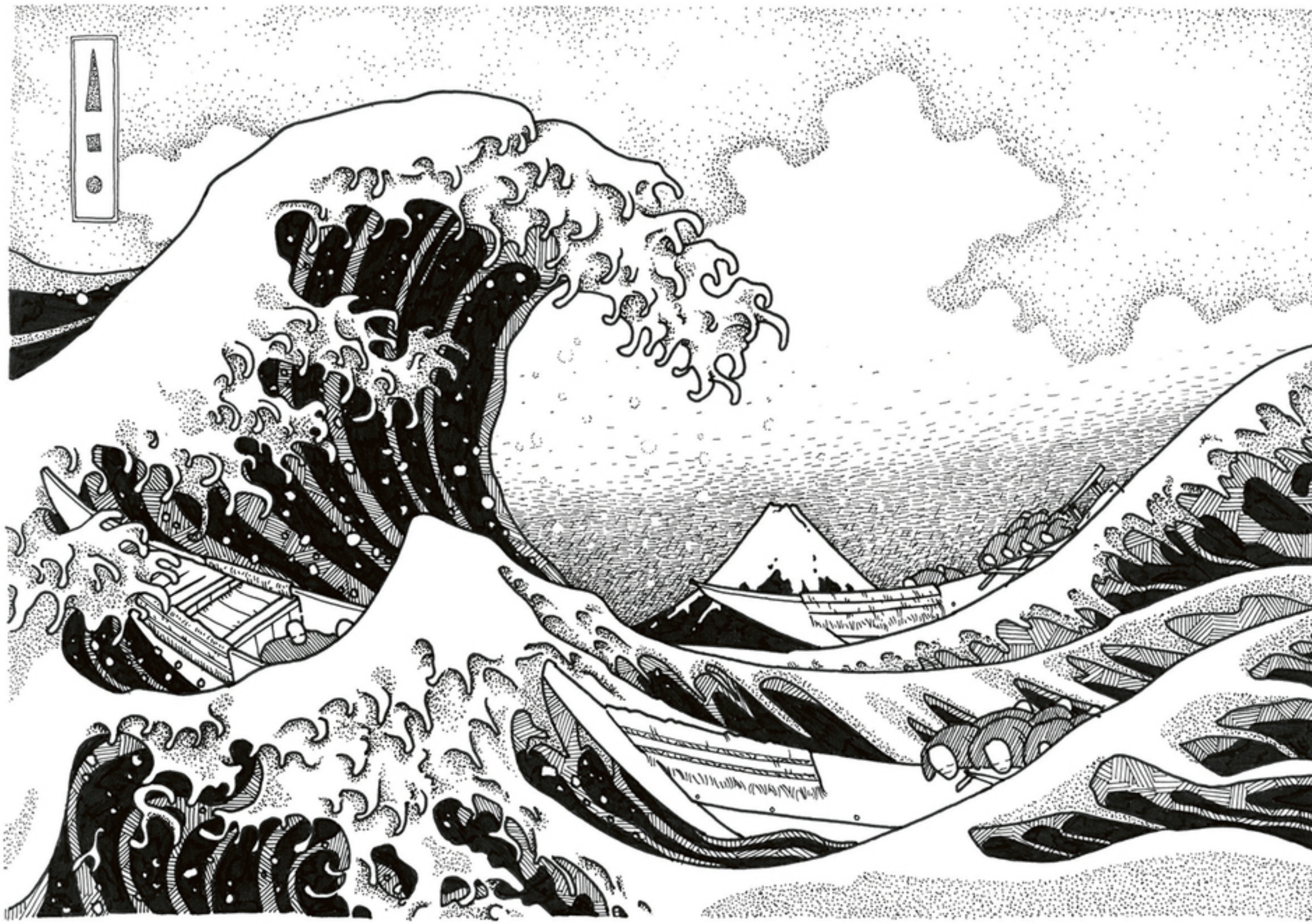

Never forget it is made out of drops!